

See discussions, stats, and author profiles for this publication at: <https://www.researchgate.net/publication/301693810>

Why are brittleness and fracability not equivalent in designing hydraulic fracturing in tight shale gas reservoirs

Article in Petroleum · March 2016

CITATION

1

READS

2,237

1 author:



Petroleum SWPU

Southwest Petroleum University

427 PUBLICATIONS 108 CITATIONS

[SEE PROFILE](#)



Review article

Why are brittleness and fracability not equivalent in designing hydraulic fracturing in tight shale gas reservoirs



CrossMark

Mao Bai

Geomechanics Consultant, Houston, USA

ARTICLE INFO

Article history:

Received 22 December 2015

Accepted 7 January 2016

Keywords:

Brittleness
Fracability
Rock stiffness
Rock strength
Formation confinement
Horizontal well landing interval

ABSTRACT

With respect to brittleness, it is about the type of material and its related strength. In comparison with ductile material under load, brittle material has a relatively shorter plastic deformation and responds dominantly by the elastic deformation. With respect to fracability, it is about the rock failure under the ultimate rock strength in either brittle or ductile formation. In comparison, the higher fracable formation should have smaller formation strength than that of the lower fracable formation. In consequence, it is not certain that the brittle formation is easy to fracture than the ductile formation since brittle formation may have greater strength than ductile formation even though the exceptions may exist.

More complications arise when evaluating the responses of subsurface formation in great depth to the formation types (e.g. brittle formation or ductile formation). Under this condition, the impact of confinement on the fracability cannot be ignored. In general, the formation subject to higher confinement pressure is more difficult to fracture as the formation strength is greater. Conversely, the formation subject to lower confinement pressure is easy to fracture since the formation strength is smaller.

In view of efficient stimulation of tight shale gas reservoirs, it is unclear whether we would choose the brittle interval or the ductile interval to fracture as the strength of either interval is unknown. However, it is apparent that we should choose the formation interval with a higher fracability which is equivalent to the lower formation strength. Under the similar confinements, the lower formation strength may be indicated by the smaller unconfined compressive strength (UCS). As a result, it is advisable that the most fracable interval is the one with lowest UCS.

When evaluating the present technology, the formation brittleness should no longer be the associated subject matter as we are unclear about its role to improve the fracability of the tight formation. Disassociating the brittleness with the fracability enables us to focus on identifying the true mechanisms of efficient fracturing of tight shale gas reservoirs.

With the objective review and sensible definition of brittleness used in the present petrophysical field to identify the desirable fracturing intervals, the paper presents the ambiguities of using the brittleness to define the formation fracability and points out that the formation brittleness can be unrelated to the formation fracability. As an alternative approach, the paper provides an effective method to define the most fracable formation intervals in designing the hydraulic fracturing in tight shale gas formations.

Copyright © 2016, Southwest Petroleum University. Production and hosting by Elsevier B.V. on behalf of KeAi Communications Co., Ltd. This is an open access article under the CC BY-NC-ND license (<http://creativecommons.org/licenses/by-nc-nd/4.0/>).

E-mail address: mao-bai@excite.com.

Peer review under responsibility of Southwest Petroleum University.



Production and Hosting by Elsevier on behalf of KeAi

1. Introduction

As world conventional hydrocarbon resources have reduced rapidly in recent years, unconventional hydrocarbon resources are gradually taking the central stage in all phases of exploitation from exploration to production. The key parameter that separates the unconventional resources in shale from conventional resources in sandstone is the formation permeability (k) with the common divider of 0.1 md, with $k > 0.1$ md for conventional reservoirs and $k < 0.1$ md for unconventional reservoirs [1]. The key method for producing from unconventional shale formations with ultralow permeability is to hydraulically fracture the tight formation with the assistance from connected natural fractures.

Based on fracture mechanics, it appears that a more brittle formation is easier to fracture [2]. As a result, identifying the brittle zones in unconventional reservoirs to achieve effective fracturing has become the focus of current research. A variety of definitions of brittleness has arisen from various disciplines which promotes the development of empirical relations between formation brittleness and formation mechanical properties, such as the correlation of Young's modulus and Poisson's ratio.

The empirical correlation such as developed by Rickman et al. [3] is convenient to use as a brittleness index log with reference to other wireline logs to assist in locating the preferred injection intervals. Brittleness is an important property that controls the failure process as discussed by Van Dam et al. [4]. Alassi et al. [5] pointed out that although rock material is considered brittle in general, many rocks show less brittle and more plastic behaviour at high stress conditions. Rock brittleness has been considered an important geomechanics parameter in the pool of petrophysical – geomechanical factors for stimulating unconventional reservoirs [6].

These empirical methods, however, have their defects of frequently neglecting the true mechanisms of effective fracturing. The controversial debates over the brittleness and fracability even for their respective definitions have intensified in recent years. For example, the negative relationship between Young's modulus and Poisson's ratio may be appropriate for certain materials. The generalization of the relation by associating it with brittleness can be dangerous. Another important but controversial question is whether the brittleness should be related to the rock strength (UCS) instead of to the rock stiffness (Young's modulus). Finally, the brittleness and fracability appear to be simple terms to relate to the stimulation effectiveness. However, the complication of brittleness may largely overshadow its usefulness in achieving the desired fracability, and the effective fracability could be determined without relating to the brittleness. The purpose of the present paper is to identify the complications of brittleness and to propose an effective method in determining the fracability to stimulate the unconventional tight reservoirs without resorting to brittleness.

2. Review of current brittleness approach

Based on the laboratory ultrasonic measurements to derive the relationship between dynamic Young's modulus and Poisson's ratio, Rickman et al. [3] proposed the following equation to evaluate the brittleness:

$$B_r = \frac{50}{7}(E - 28\nu + 10.2) \quad (1)$$

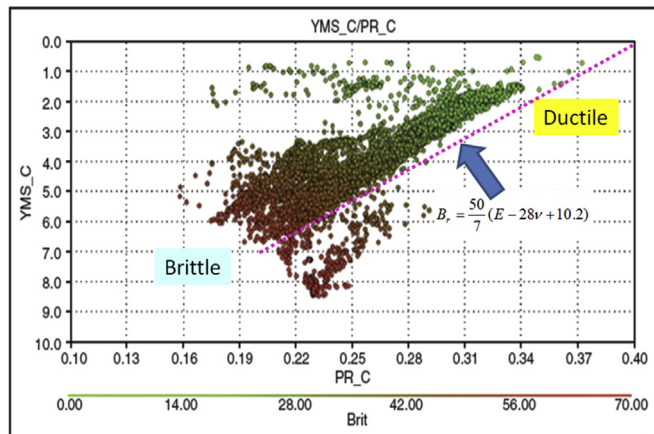


Fig. 1. Linear relationship between Young's modulus and Poisson's ratio from Eq. (1) (YMS_C unit is mpsi → psi × 10⁶ and 1 mpsi = 6.8947573 GPa; [3]).

where E is Young's modulus and ν is Poisson's ratio, both are derived from the correlations of sonic velocity logs. It can be easily proved that

- $B_r = 0$ when $E = 1$ (mpsi) and $\nu = 0.4$
- $B_r = 70$ when $E = 6.1604$ (mpsi) and $\nu = 0.2343$

where mpsi = psi × 10⁶; 1 mpsi = 6.8947573 GPa.

The data from Eq. (1) can be illustrated by the dotted pink line in Fig. 1.

The relationship between Young's modulus and Poisson's ratio to interpret formation brittleness proposed by Rickman et al. [3] in Eq. (1) has been widely used in the petrophysical domain as an indispensable geomechanical component in stimulating unconventional tight reservoirs. The workflow has been established by the practitioners in oil/gas industry to plot the brittleness index log along the perforated interval in order to identify the desired fracturing intervals.

However, Rickman et al.'s proposal raised much opposition from the geomechanics domain. The main debate is about the definition of brittleness. Using the proportion between elastic

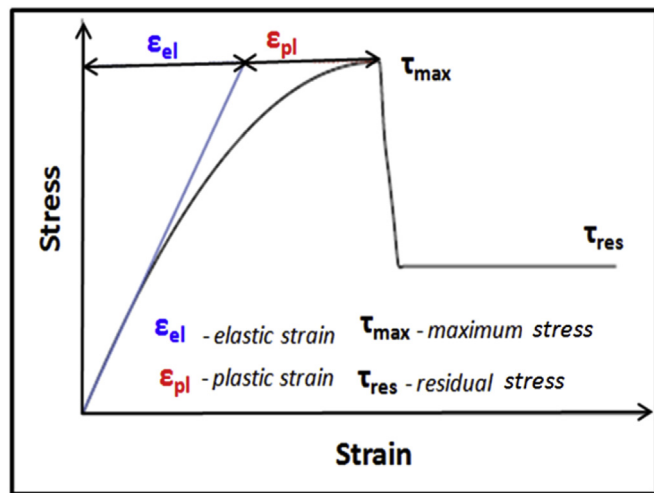


Fig. 2. Relation between stress and strain to determine the elastic strain (ϵ_{el}) and plastic strain (ϵ_{pl}) [7].

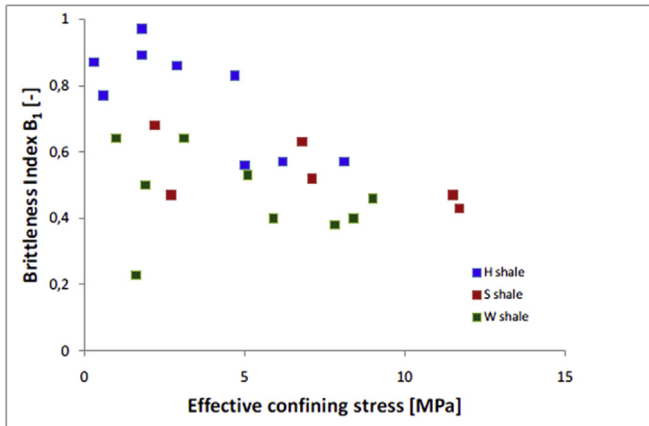


Fig. 3. Relation between brittleness defined in Eq. (2) and effective confining stress [7].

deformation and plastic deformation as well as the maximum stress (τ_{\max}) and residual stress (τ_{res}) as reference points, as shown in Fig. 2, Holt et al. [7] proposed the following equation to calculate the brittleness:

$$B_r = \frac{\varepsilon_{el}}{\varepsilon_t} \quad (2)$$

where ε_{el} is the elastic strain and ε_t is the total strain:

$$\varepsilon_t = \varepsilon_{el} + \varepsilon_{pl} \quad (3)$$

where ε_{pl} is the plastic strain.

For three types of clay-rich shale (H Shale – clay 30–85%; S Shale – clay 47%; W Shale clay 44%), Holt et al. [7] related brittleness defined in Eq. (2) to the effective confining stress as shown in Fig. 3. The apparent reversed relation between brittleness and effective confining stress exists for all shales, especially for H Shale. In other words, greater brittleness refers to smaller confining stress.

Holt et al. [7] attempted to reproduce the result from Rickman et al. [3] using laboratory ultrasonic tests under the same hydrostatic loading conditions to generate the P wave and S wave velocities. The brittleness by Rickman et al. [3] should in principle represent brittleness under the conditions where wave velocities are measured. Since wave speeds

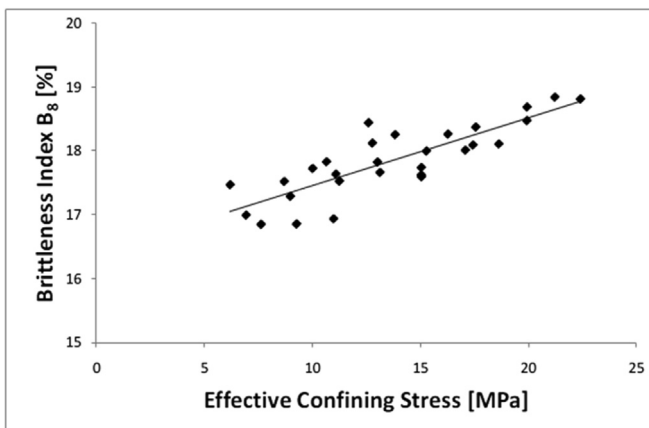


Fig. 4. Relation between brittleness defined in Eq. (1) and effective confining stress based on the ultrasonic measurements under hydrostatic loading [7].

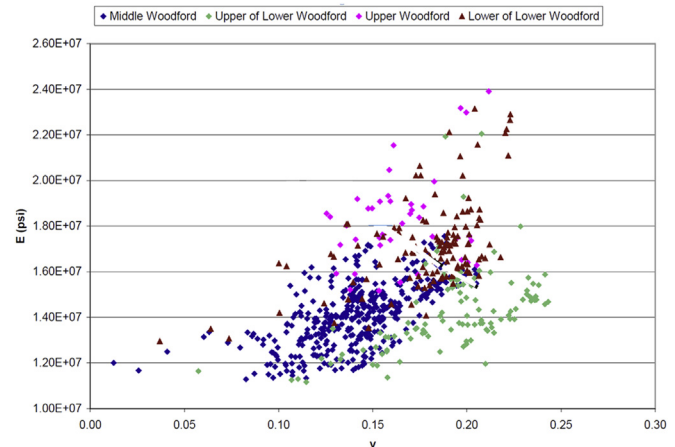


Fig. 5. Positive correlation between Young's modulus and Poisson's ratio for Woodford cases [8].

increase with increasing stress and P-wave velocity normally increases faster than S-wave velocity, one would expect the brittleness by Rickman et al. [3] to increase rather than decrease with increasing stress such as confining stress. Holt et al. [7] performed the laboratory ultrasonic tests under hydrostatic stress condition to clay-rich North Sea F Shale and confirmed the positive correlation between brittleness and confining stress, as shown in Fig. 4. It is understood that the in-situ confining stress represents the lateral stress or often horizontal stress that can be determined if the stress path is known. In general, the in-situ stress under the hydrostatic condition (stress path = 1) is extremely rare. For this reason, the result in Fig. 4 should not be considered as a general guide to the derivation of brittleness.

Miskimins [8] collected the correlations between Young's modulus and Poisson's ratio from various depths of different parts of Woodford shale intervals, and showed in Fig. 5 that a positive trend between Young's modulus and Poisson's ratio indeed exists. The trend in Fig. 5 is apparently contradictory to the trend by Rickman et al. [3] in Fig. 1 (Note: "Y" axis in Miskimins' case is in a reversed order from "Y" axis in Rickman et al.'s case).

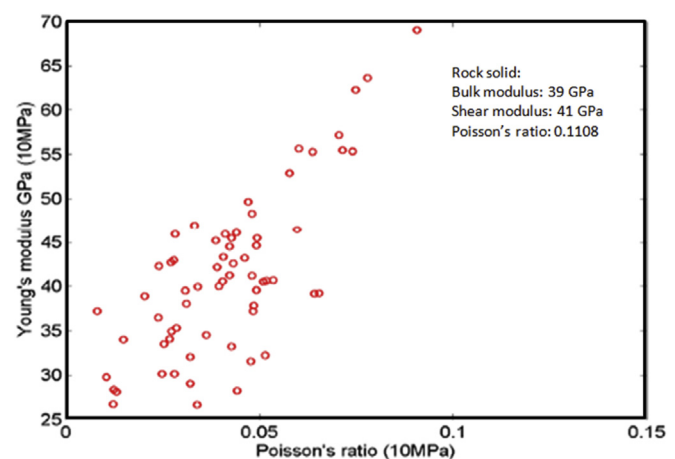


Fig. 6. Poisson's ratio is positively related to Young's modulus in fractured dry rock [9].

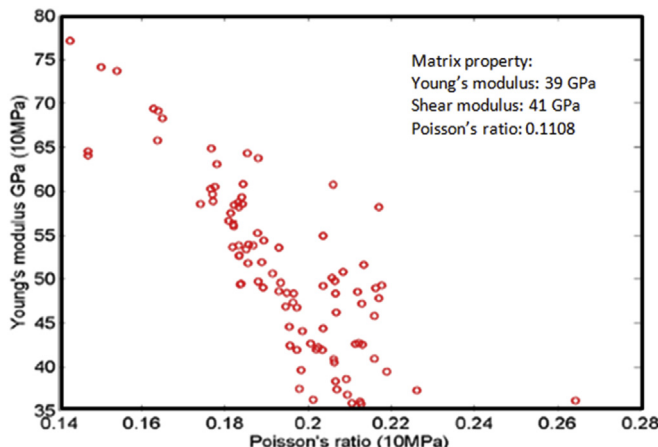


Fig. 7. Poisson's ratio is negatively related to Young's modulus in fractured wet rock [9].

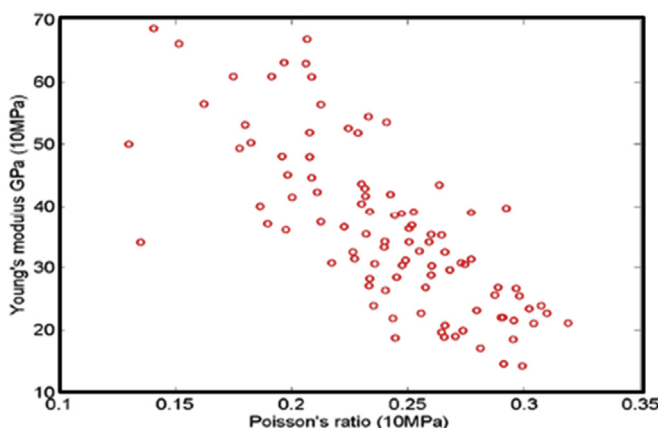


Fig. 8. The relationship between Young's modulus and Poisson's ratio is in reserve mode when the deformable rock contains fewer fractures but fractures are water saturated [9].

Zhang and Bentley [9] proposed that the fractures in the rock and their saturation status would affect the relation between Young's modulus and Poisson's ratio significantly. For the case with the fractures being dominated in the rock without saturated fluid, Fig. 6 indicates that Young's modulus has a positive relation with Poisson's ratio, similar to the case shown in Fig. 5. The rock is dry and under the effective pressure of 10 MPa. Zhang and Bentley argued that greater Poisson's ratio corresponds to larger Young's modulus while the higher Poisson's ratio is the result of fewer cracks, which leads to the larger Young modulus.

If the fractures are still pervasive but the rock is water saturated, then the relationship between Young's modulus and Poisson's ratio is reversed, as shown in Fig. 7 [9]. The greater Poisson's ratio is related to the smaller Young's modulus. The fewer cracks are conversely the result of high pressure.

If the deformable rock is not heavily fractured and if the rock is water saturated, the reverse relation between Young's modulus and Poisson's ratio with certain degree of smearing is observed (Fig. 8).

Altindag [10] defined the brittleness as a property of materials that rupture or fracture with little or no plastic deformation. Altindag believed that brittleness measures the relative preference of a material to two competing mechanical responses: deformation and fracture in the process of ductile–brittle transition.

The equations calculating brittleness are largely empirical. The following criterion of brittleness has been used widely [11–14]; and [15]:

$$B_r = \frac{\sigma_c}{\sigma_t} \quad (4)$$

where σ_c is the unconfined compressive strength (UCS) and σ_t is the tensile strength.

B_r in Eq. (4) is a dimensionless number. It means that if the rock strength under no confinement (i.e., UCS) is significant, the rock is brittle. If no information about the tensile strength of the rock is available, it can be assumed to be 1/10th of UCS.

Instead of the simple ratio in Eq. (4), Altindag [10] proposed the alternative brittleness as follows:

$$B_r = \frac{\sigma_c \times \sigma_t}{2} \quad (5)$$

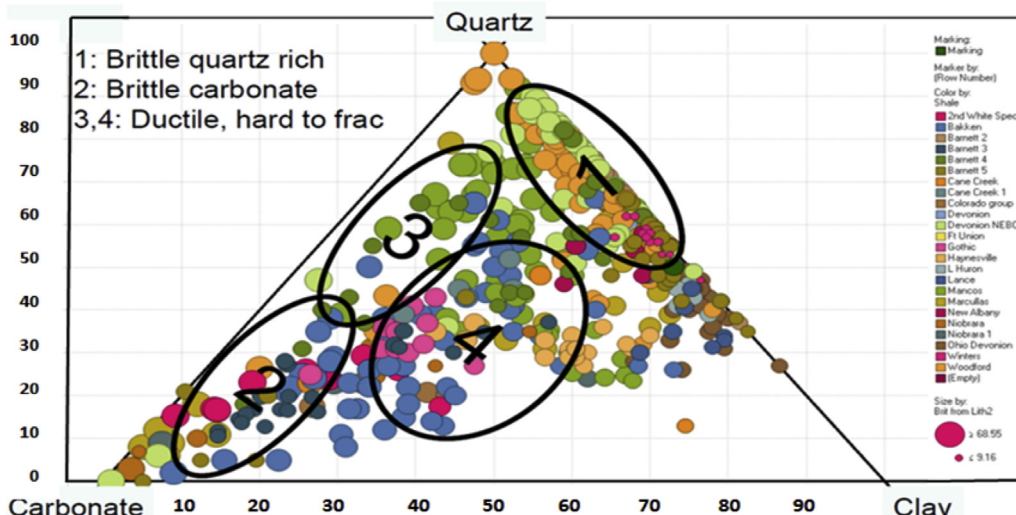


Fig. 9. Brittle shale is either quartz rich or carbonate rich, otherwise it is ductile [3].

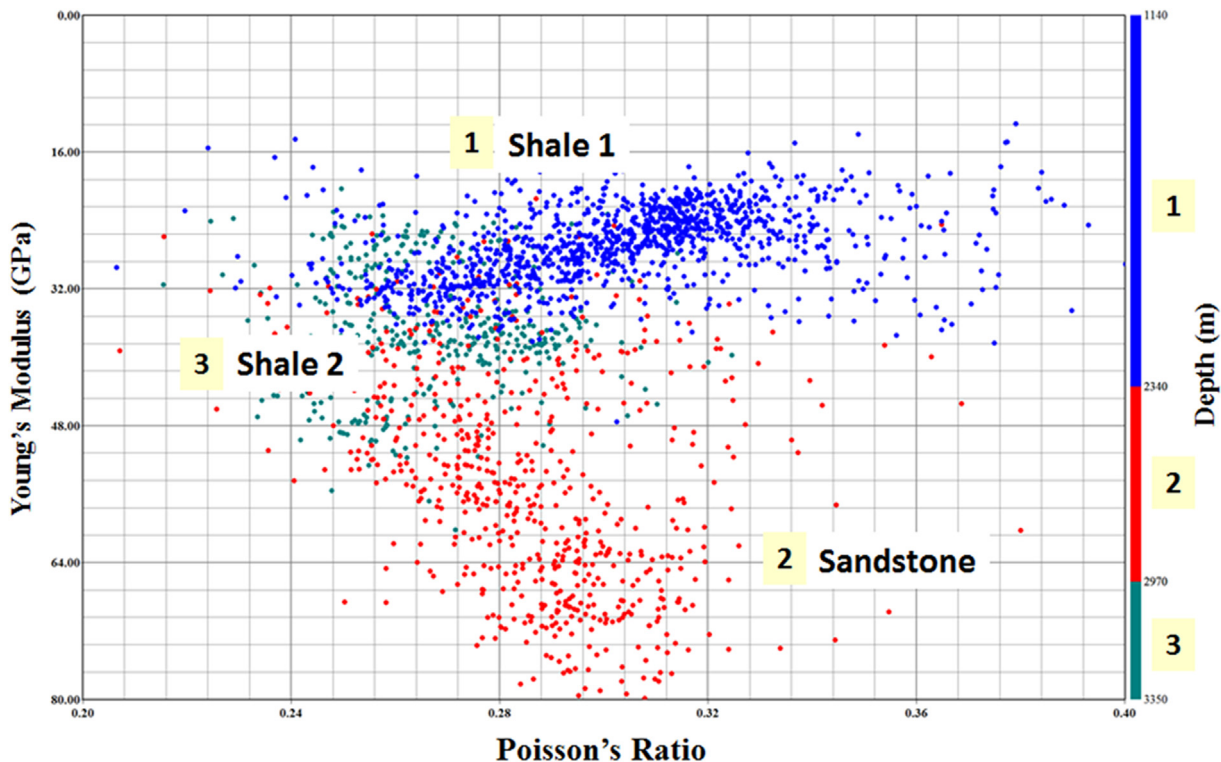


Fig. 10. Cross plot between Young's modulus and Poisson's ratio showing negative relation in the upper shale and positive relation in reservoir sands. The data from the lower shale has little impact in the relationship chart.

Using the average area concept to calculate the brittleness shown in Eq. (5), Altindag [10] considered the brittleness definition in Eq. (5) as a better one because it showed a strong correlation to the specific energy with the improved application in describing cutting efficiency.

With respect to the influence of mineralogy on brittleness of the shale, Rickman et al. [3] claimed that shale is brittle if it is quartz rich or carbonate rich. Conversely, the shale is ductile if it is clay rich, as depicted in Fig. 9.

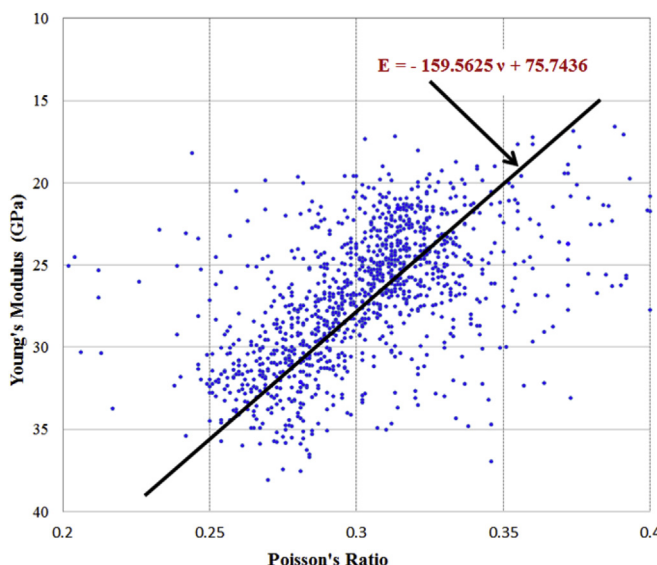


Fig. 11. Negative linear relation between Young's modulus and Poisson's ratio for the shallow shale section in Fig. 10.

Jarvie [16] proposed the relation between brittleness and shale mineralogy as follows:

$$\text{Brittleness} = \frac{\text{Quartz}}{\text{Quartz} + \text{Carbonate} + \text{Clay}} \quad (6)$$

Jarvie assumed that the content of quartz dictates the brittleness of the shale.

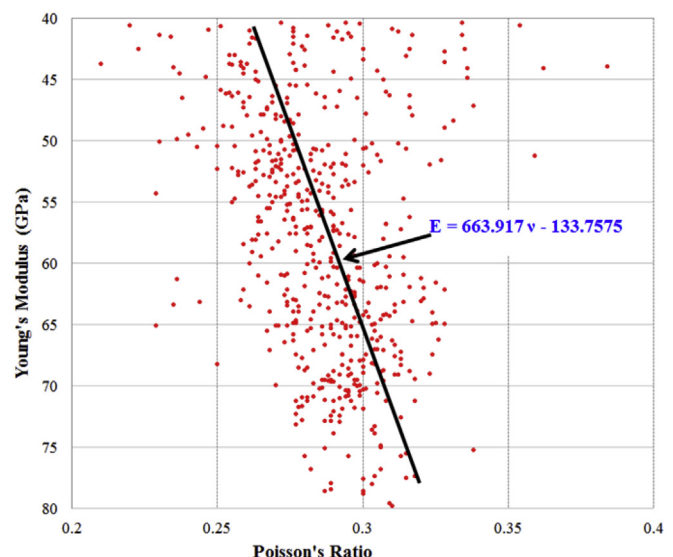


Fig. 12. Positive linear relation between Young's modulus and Poisson's ratio for the sandstone section in Fig. 10.

Table 1

Brittleness definition in current literature Ref. [17].

Formulae	Variables	Methods	References
$B_{r1} = (H_m - H)/K$	H-hardness, H_m -micro hardness, K-bulk modulus	Hardness test	Honda and Sanada [18]
$B_{r2} = q\sigma_c$	q-percent of debris, σ_c -compressive strength	Impact test	Protodyakonov [19]
$B_{r3} = \varepsilon_{ux}$ (100%)	ε_{ux} -unrecoverable axial strain	Stress-strain test	Andreev [20]
$B_{r4} = (\varepsilon_p - \varepsilon_r)/\varepsilon_p$	ε_p -peak strain, ε_r -residual strain	As above	Hajibolmajid and Kaiser [21]
$B_{r5} = (\tau_p - \tau_r)/\tau_p$	τ_p -peak shear stress, τ_r -residual shear stress	As above	Bishop [22]
$B_{r6} = \varepsilon_r/\varepsilon_t$	ε_r -recoverable strain, ε_t -total strain	As above	Hucka and Das [23]
$B_{r7} = W_r/W_t$	W_r -recoverable strain energy, W_t -total strain energy	As above	As above
$B_{r8} = \sigma_c/\sigma_{ten}$	σ_c -compressive strength, σ_{ten} -tensile strength	UCS and Brazilian tests	As above
$B_{r9} = (\sigma_c - \sigma_{ten})/(\sigma_c + \sigma_{ten})$	As above	As above	As above
$B_{r10} = (\sigma_c\sigma_{ten})/2$	As above	As above	Altindag [10]
$B_{r11} = (\sigma_c\sigma_{ten})^{0.5}/2$	As above	As above	As above
$B_{r12} = H/K_{IC}$	H-hardness, K_{IC} -fracture toughness	Hardness and fracture toughness tests	Lawn and Marshall [24]
$B_{r13} = c/d$	c-crack length, d-indent size	Indentation test	Sehgal et al. [25]
$B_{r14} = P_{inc}/P_{dec}$	P_{inc} -increment force, P_{dec} -decrement force	As above	Copur et al. [26]
$B_{r15} = F_{max}/P$	F_{max} -max. force, P-related penetration	As above	Yagiz [27]
$B_{r16} = H^*E^* K_{IC}^2$	H-hardness, E-Young's modulus, K_{IC} -fracture toughness	Hardness, stress-strain, and fracture toughness tests	Quinn and Quinn [28]
$B_{r17} = 45^\circ + \phi/2$	ϕ -internal friction angle	Mohr-Coulomb analysis	Hucka and Das [23]
$B_{r18} = \sin\phi$	As above	As above	As above
$B_{r19} = (E_n + v_n)/2$	E_n -normalized Young's modulus, v_n -normalized Poisson's ratio	Sonic logging data analysis	Rickman et al. [3]
$B_{r20} = W_{qtz}/W_t$	W_{qtz} -weight of quartz, W_t -total mineral weight	Mineralogy or XRD analysis	Jarvie et al. [16]
$B_{r21} = (W_{qtz} + W_{dol})/W_t$	As above, also W_{dol} -weight of dolomite	As above	Wang and Gale [29]
$B_{r22} = (W_{QFM} + W_{carb})/W_t$	W_{QFM} -weight of quartz, feldspar and mica; W_{carb} -weight of carbonates, W_t -total mineral weight	As above	Jin et al. [17]

Buller et al. [30] proposed the equation to calculate the $Frac_{index}$ (i.e., fracability) as:

$$Frac_{index} = \frac{B_r}{TIV} \quad (7)$$

where B_r is the brittleness defined by Rickman et al. [3] in Eq. (1), while TIV is the transverse interval velocity and:

$$TIV = \frac{DTS_{slow}}{DTS_{fast}} \quad (8)$$

where DTS_{slow} is the slow sonic shear travel time and DTS_{fast} is the fast sonic shear travel time, respectively.

Hucka and Das [23] proposed a simple method to calculate the brittleness using the single factor of internal friction angle as follows:

$$B_r = \sin\phi (0 \leq \phi \geq 90) \quad (9)$$

where ϕ is internal friction angle. From Eq. (9), it is seen that the larger the friction angle, the greater the brittleness.

Referring to the unconfined compressive strength and tensile strength, Hucka and Das [23] presented another equation of brittleness:

$$B_r = \frac{C_0 - \sigma_T}{C_0 + \sigma_T} \quad (10)$$

where C_0 is the unconfined compressive strength (UCS) and σ_T is tensile strength.

Baron et al. [31] presented the brittleness using the energy terms as follows:

$$B_r = \frac{W_{el}}{W_{tot}} \quad (11)$$

where W_{el} is the elastic energy while W_{tot} is the total energy.

Using peak shear strength (τ_{max}) and residual shear strength (τ_{res}), Bishop [22] defined the brittleness as:

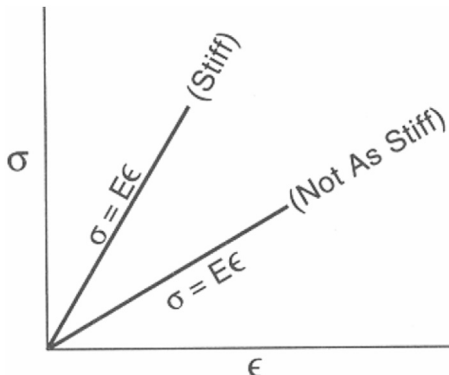


Fig. 13. A stiffer material has a greater Young's modulus E.

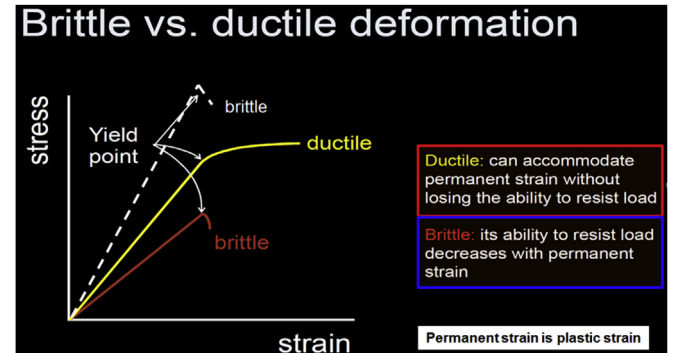


Fig. 14. Material failure in brittle mode and ductile mode.

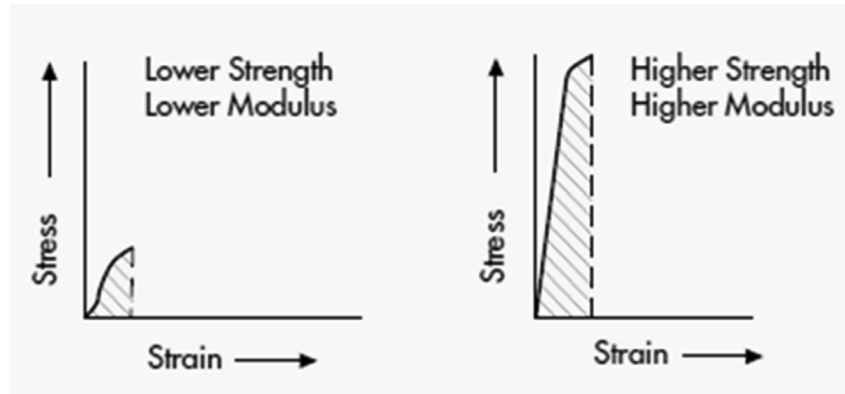


Fig. 15. Brittle rock failure for low stiffness and low strength rock as well as for high stiffness and high strength rock [32].

$$B_r = \frac{\tau_{\max} - \tau_{\text{res}}}{\tau_{\max}} \quad (12)$$

Hajabdolmajid and Kaiser [21] proposed the brittleness in the following equation:

$$B_r = \frac{\varepsilon_{p^*} - \varepsilon_{s^*}}{\varepsilon_{s^*}} \quad (13)$$

where ε_{p^*} is the plastic strain at failure while ε_{s^*} is the specific strain beyond failure.

Employing the stress as primary variable, Ingram and Urai [33] defined the brittleness in the following equation:

$$B_r = \left(\frac{\sigma_{v,\max}}{\sigma_v} \right)^b \quad (14)$$

where $\sigma_{v,\max}$ is the maximum previous experienced effective vertical stress, σ_v is the current effective vertical stress, and b is the empirical constant.

Using the static data from rock mechanical testing [34,35], Yang et al. [36] observed that the brittleness defined by Holt et al. [7] in Eq. (2) showed the reversed relationship with the confinement pressure, as observed by Holt et al. [7]. On the other hand, the brittleness defined by Eq. (2) did not show an apparent relationship to Young's modulus and Poisson's ratio, according to the report by Yang et al. [36].

With reference to various definitions of brittleness as described above, sensible ones are those related to rock strength (e.g., tensile, shear or compressive strength) and rock failure (e.g., permanent failure or plastic deformation). Other non-strength or non-failure related definitions of brittleness have been suggested but may have not been physically verified.

From the data of a well in Gulf of Mexico (GOM, data from the published domain), Fig. 10 shows the cross plot between Young's modulus and Poisson's ratio for sandstone and shale. The blue dots represent values from the upper overburden shale formation while the red dots represent values from the reservoir sandstone section. The green dots represent the lower shale formation.

The approximated negative linear section between Young's modulus and Poisson's ratio is from Section 1 of the shallow shale (Section 1, blue dots). Conversely, Sandstone (red dots) in Section 2 shows an approximately positive linear relationship between Young's modulus and Poisson's ratio. For the deep shale (Section 3, green dots), the relationship between Young's modulus and Poisson's ratio becomes unclear. It appears that the data from the deep shale are clustered at the intersection between the shallow shale and sandstone sections and further are overshadowed by the two strong linear relationships.

For the shallow shale section, the negative linear relationship between Young's modulus and Poisson's ratio can be represented in Fig. 11. The trend is consistent with the one proposed by Rickman et al. [3] shown in Fig. 1 (note: 1 mpsi = 6.8947573 GPa). For

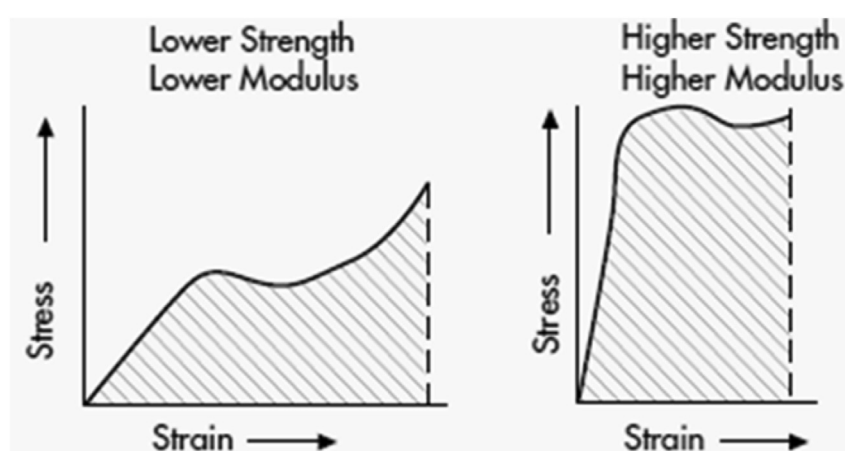


Fig. 16. Ductile rock failure for low stiffness and low strength rock as well as for high stiffness and high strength rock [37].

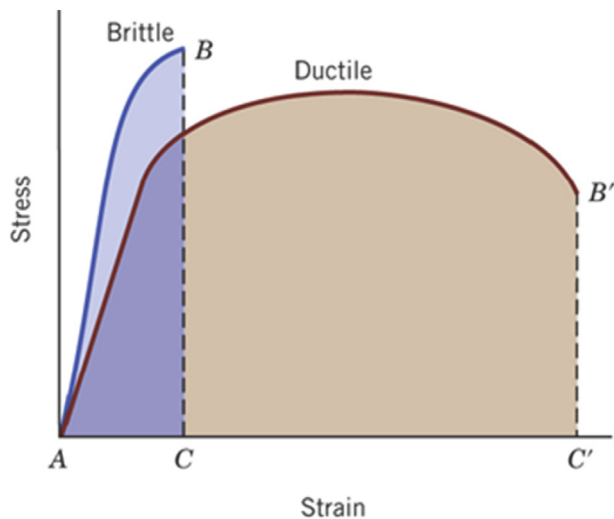


Fig. 17. Strain from ductile failure is much greater than strain from brittle failure [38].

sandstone section, the positive linear relationship between Young's modulus and Poisson's ratio is depicted in Fig. 12. It may be speculated that the relation between Young's modulus and Poisson's ratio proposed by Rickman et al. [3] may be relevant only to the shallow shale formations.

Jin et al. [17] provided a comprehensive listing of current brittleness definitions and methods, which can be viewed in Table 1.

3. Brittleness and ductility are related to rock strength

The definitions of stiffness and strength can be confusing. A material may be stiff and strong, but this statement cannot be generalized because some stiff materials may also be weak. From the point of view of rock mechanical testing, strength refers to a load carrying capability, which is related to the material failure, while stiffness refers to a deflection capability, which is related to a material property.

The definition of stiffness is the ability of a material to resist the non-permanent (or elastic) deformation. For example, Young's modulus (E), also known as the elastic modulus, is a measure of the stiffness of an elastic material or a material at the elastic stage [see stress (σ) – strain (ϵ) relationship in Fig. 13]. There is no indication of material failure from Young's modulus (E) alone (Fig. 13).

Brittleness, on the other hand, is the ability of a material to resist permanent (or inelastic) deformation. Permanent deformation represents material failure. When the material changes from the elastic stage to the plastic stage, the material is subjected to failure or the material is in dilation. For brittle failure, however, the period of plastic deformation is short and brief. If the period of plastic deformation is long, the material is subjected to ductile failure. As shown in Fig. 14, the difference between brittle material and ductile material is the duration of the ability to resist the permanent deformation (plastic strain) or ultimate load. It is noted that brittleness is independent of Young's modulus.

The bottom line is that elasticity and plasticity are related to rock mechanical properties while brittleness and ductility are related to the rock mechanical strength at failure. In other words,

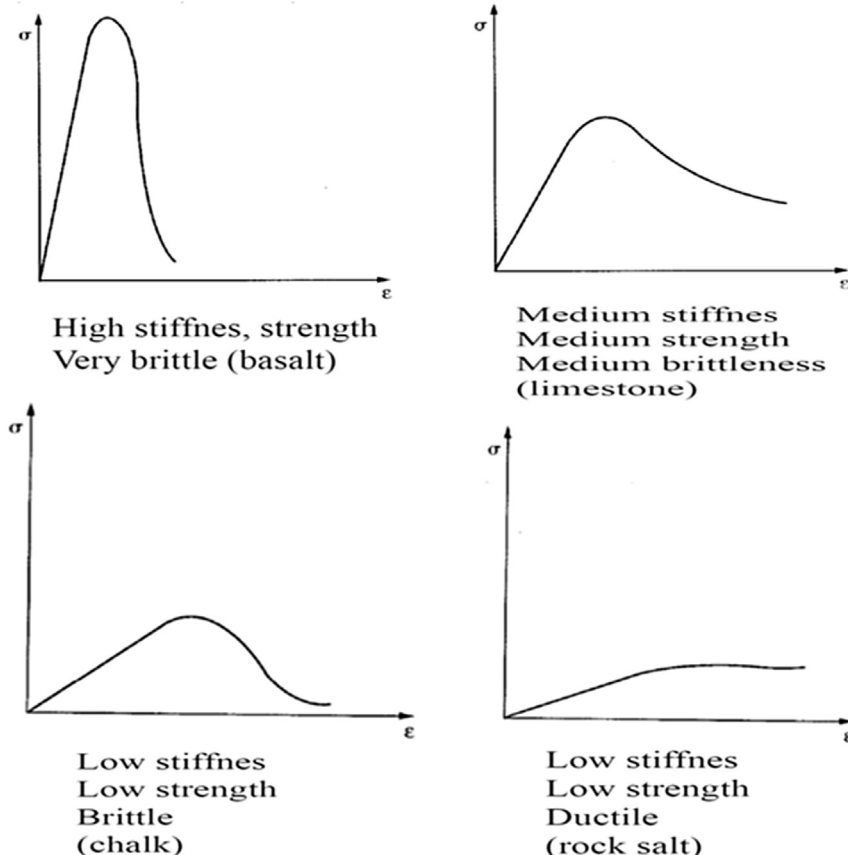


Fig. 18. Stiffness, strength, brittleness and ductility can have different combinations for different rocks [39].

brittle rock failure implies that rock is still largely elastic but may be partially plastic. By the same token, ductile rock failure indicates that rock is largely plastic but may be partially elastic. Elastic – brittle and plastic – ductile are often used as equivalent terms in literature. However, the subtle but important differences among them must be recognized.

As in Fig. 15 [37], brittle rock failure can occur with both low strength and low modulus (stiffness) as well as with high strength and high modulus.

Similarly, the ductile rock failure can occur with both low stiffness and low strength rock as well as with high stiffness and high strength rock, as shown in Fig. 16 [37].

The comparison between the brittle failure in Fig. 15 and ductile failure in Fig. 16 points out an important difference between these two failures, that is, the deformation, or strain, from brittle failure is much smaller than that from ductile failure. This difference was recognized by MPE [38] for different materials (alloys, ceramics and polymers) as shown in Fig. 17.

Therefore, there is no definite rule that more brittle rock is stiffer and stronger while more ductile rock is softer and weaker. As demonstrated by Hudson and Harrison [39]; the rock stiffness and strength vary with different rocks regardless of whether it is brittle failure or ductile failure (Fig. 18).

As illustrated in Fig. 19 [40], brittle failure is dominated by the elastic deformation with a small portion of plastic deformation from the rock mechanical testing. The opposite is true for ductile failure which is dominated by plastic deformation.

As reviewed in Section 3, definition of brittleness is not unique due to the physical complexity of rock failure. While multiple definitions of brittleness should be permitted, a simple check of the definition is necessary to constrain the brittleness in the concept of rock failure rather than in other mechanisms. For example, most of brittleness definitions reviewed by Jin et al. shown in Table 1 are related to the rock strength and associated rock failure. As a result, these definitions of brittleness are generally acceptable. However, the definitions of brittleness by methods 19, 20, 21 and 22 in Table 1 are related to none rock strength factors such as Young's modulus and rock mineralogy,

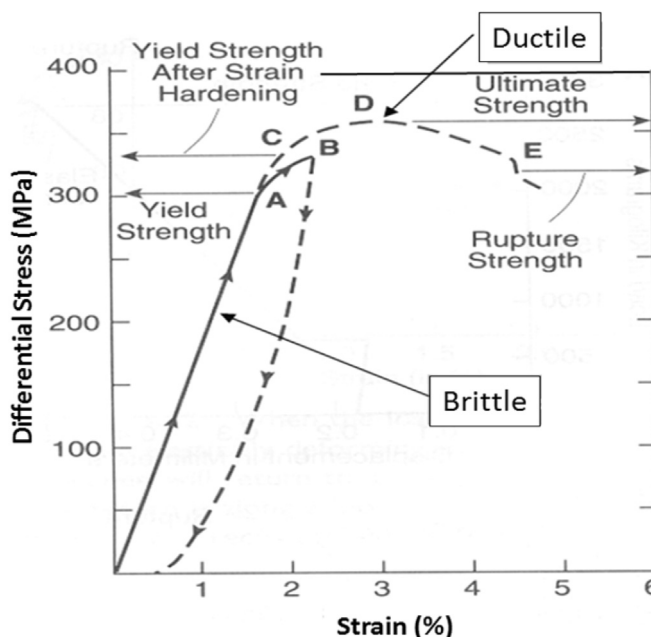


Fig. 19. Brittle failure and ductile failure from rock mechanical tests [40].

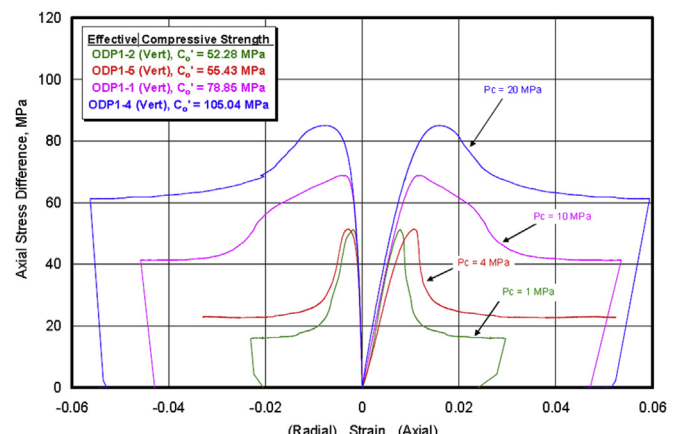


Fig. 20. Axial stress difference (axial) versus strain (axial and radial) relations from four triaxial tests [41].

which are not acceptable as the strength is different from the stiffness even though they are both mechanical properties, while the mineralogy is a chemical property which deviates from the original definition of brittleness (i.e., a mechanical term).

4. Impact of confinement on brittleness and ductility

The impact of confinement on the rock brittleness was pointed out by Holt et al. [7] as seen in Figs. 3 and 4. Since the brittleness is strongly the function of confinement conditions, we focus on the more in-depth discussion about the relationship between brittleness and confinement.

The critical transition from brittle failure to ductile failure is an important point to be determined from the stress strain curve of the rock mechanical test. A common misconception is that this critical brittle–ductile transition point can be determined from the relationship between axial stress difference and strain by capturing the slope change of the stress–strain relation. As shown in the stress–strain curves from four triaxial tests under four different confinement pressures in Fig. 20 [41], we cannot determine if there are any of these critical brittle–ductile transition points. At the lower confinement pressure ($P_c = 1 \text{ MPa}$ and $P_c = 4 \text{ MPa}$), the rock failure appears to be brittle. When the confinement pressure was increased to 10 MPa , the rock failure becomes ductile. There was a slight

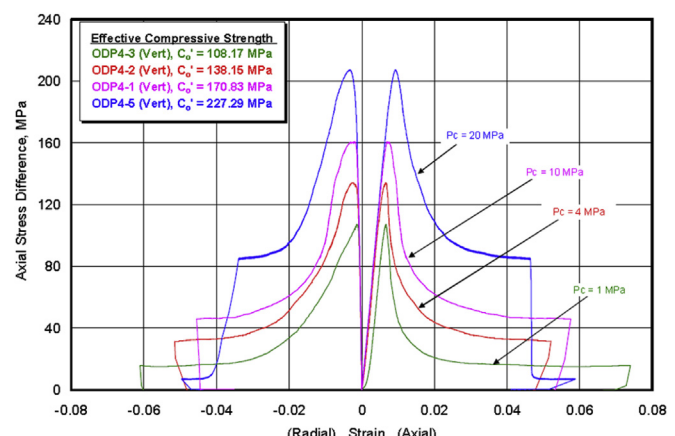


Fig. 21. Axial stress difference versus strain relations (axial and radial) from four triaxial tests using high strength rocks Ref. [41].

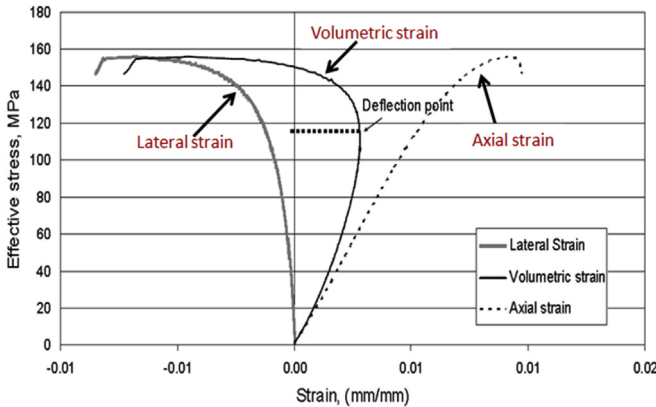


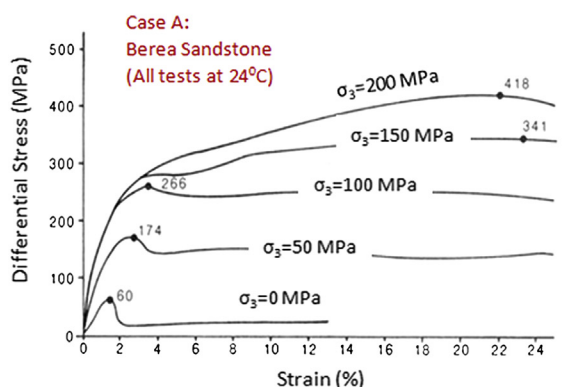
Fig. 22. Axial stress difference versus various strains from one triaxial test [42].

drop of ductility when the confinement pressure was increased to 20 MPa. However, Lutz et al. [41] presented another group of tests using the higher strength rocks (i.e., about doubled effective compressive strength compared to the previous group), as shown in Fig. 21. It can be seen that all rock failures were brittle in nature regardless of the significant changes in the confinement pressures.

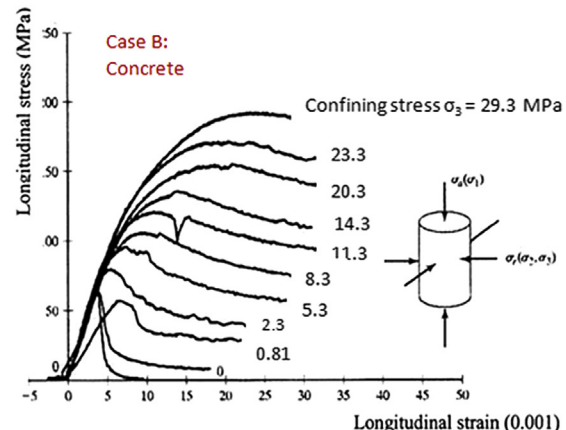
Determining whether the material is subjected to dilation or not can only be done with the help of the relationship between

axial stress difference and volumetric strain. As shown in Fig. 22 [42], dilation did not occur until the volumetric strain passed the deflection point. The negative change of volumetric strain represents the domination of radial strain over axial strain that indicates rock dilation under compressive loading.

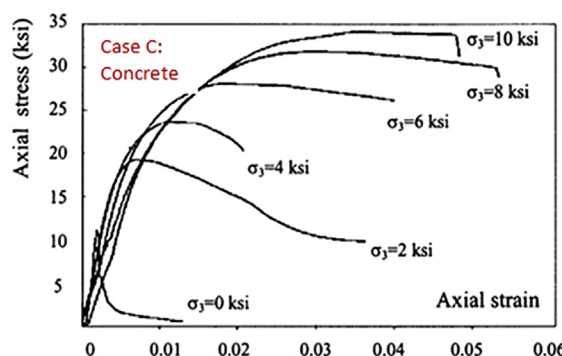
The scenarios in Figs. 20 and 21 indicate that the rock appears to be stiffer as the confinement pressure increases, i.e., Young's modulus increases as the confinement pressure increases. We intend to draw a similar conclusion for the brittleness even though it is not conclusive in Fig. 20 and even less certain in Fig. 21. Four stress-strain relation cases are presented in Fig. 23, while Case (A) was from rock testing (i.e., Berea sandstone) and Cases (B), (C) and (D) were from concrete testing. It is almost certain that the lower confinement pressure contribute to the more brittle material failure, and the material failure becomes more ductile as the confinement increases. It is of interest to note from Fig. 23 that material stiffness in the form of Young's modulus derived from the four groups of tests varies from case to case as: a) the stiffness varies greatly in the positive fashion, i.e., stiffness increases as confinement increases in Case (A); b) the stiffness has little change in Case (B) except for the 0.81 MPa confinement case; c) the stiffness varies in the negative manner, i.e., stiffness decreases as the confinement increases in Case (C); and d) the stiffness has no change in Case (D). The three cases for concrete testing in Fig. 23 demonstrate that the Young's modulus appears to be not related to the confinement pressures because that the material is not a real rock with the porosity being nearly zero. In contrast, the positive responses of variations in



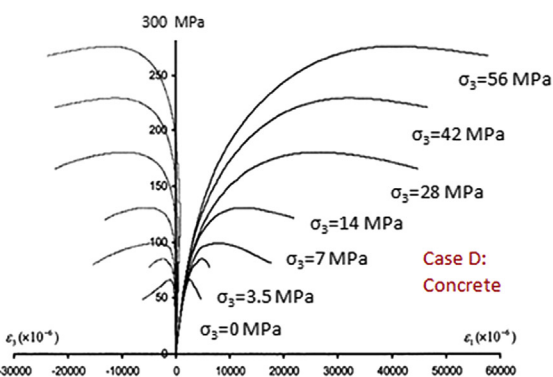
(A) Stress – strain relations under various confinements [40]



(B) Stress – strain relations under various confinements [44]



(C) Stress – strain relations under various confinements [43]



(D) Stress – strain relations under various confinements [44]

Fig. 23. Four cases of stress-strain relations under various confinements [43,44].

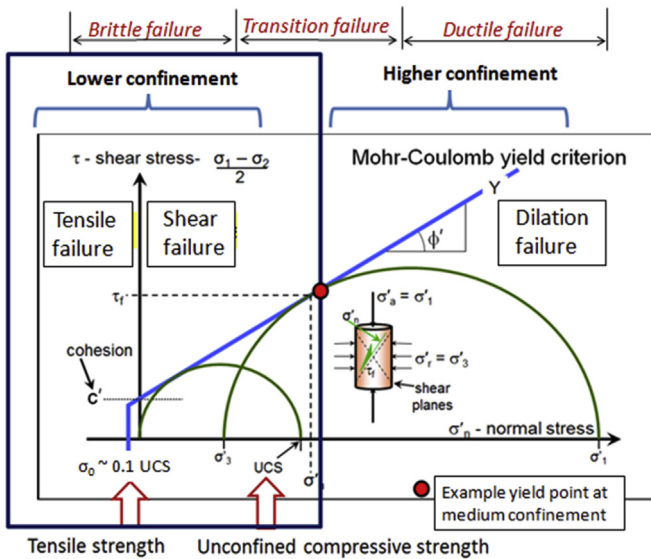


Fig. 24. Example yield point is the cutoff value in the transition failure between brittle (lower confinement) and ductile (higher confinement) rock failures in the Mohr–Coulomb chart.

Young's modulus for the real rock [e.g., sandstone in Case (A) of Fig. 23] with respect to the increase in the confining pressures are the result of increasing rock porous space compaction under loading.

It is understood that more brittle rock failure occurs at a lower confinement condition while more ductile failure occurs at a higher confinement condition, as demonstrated by Fig. 24 for the conceptual two-sample testing case, and by Fig. 25 for the actual six-sample testing case [45].

The transition point from brittle rock failure to ductile rock failure cannot be easily captured since the transition is gradual. The case presented by Kirby [46] using the chart between stress difference and confining pressure in Fig. 26 supports the cases in Figs. 24 and 25 that the brittle rock is under a lower confinement and the ductile rock is under a higher confinement.

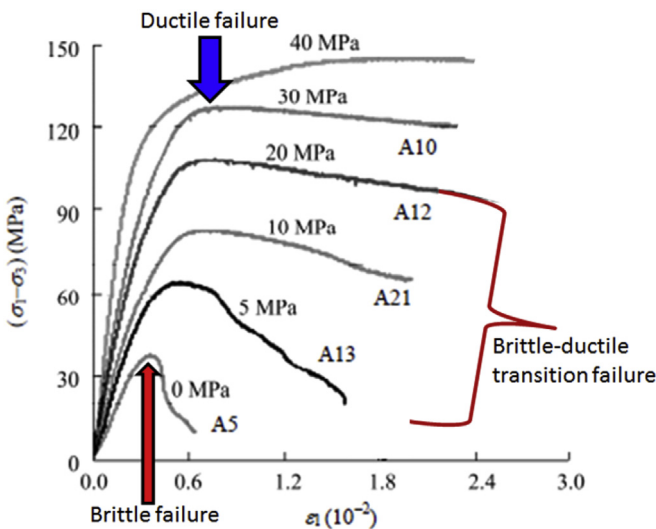


Fig. 25. Lower confinement leads to more brittle failure while higher confinement leads to more ductile failure. The brittle–ductile transition is gradual [27].

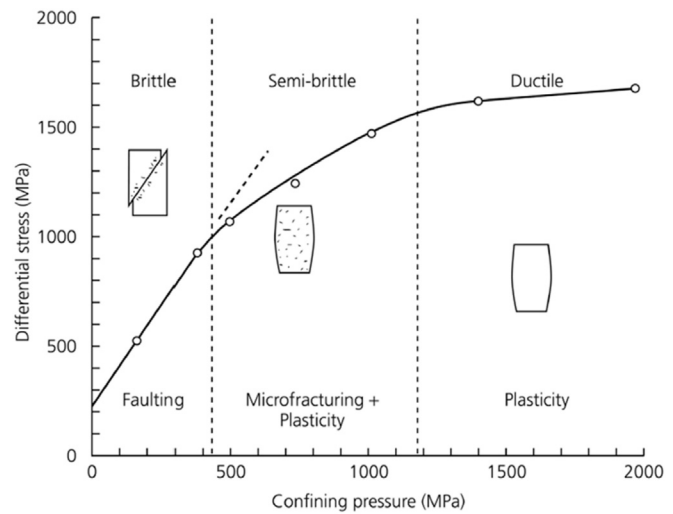


Fig. 26. It may be commonly known that brittle failure occurs in the low confinement condition while ductile plastic failure occurs in the high confinement condition [46].

Based on this concept described in Figs. 24–26, Suppe [32] examined rock strength in quartz rich sedimentary rocks with hydrostatic pore pressure and made assumptions that the brittle rock failure occurred in the under-deformed shallower region, while the ductile rock failure occurred in the deformed deeper formation (Fig. 27 quoted from Suppe-1985 with modification). The brittle–ductile transition point is at the intersection between bilinear lines for brittle rock strength in the under-deformed region and a nonlinear curve for ductile rock strength in the deformed region.

5. Formation fracability – unrestricted fracturing

Previous discussion indicates that rock brittleness and ductility are not related to the rock stiffness (e.g., Young's

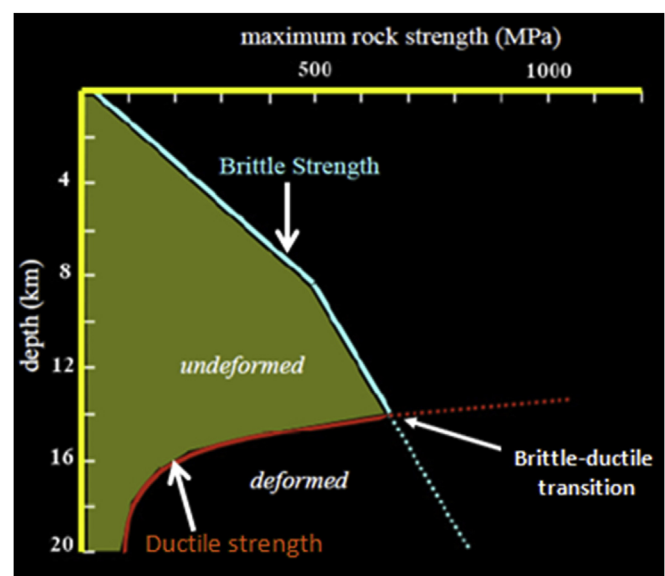


Fig. 27. Brittle rock in the undeformed shallower depth versus ductile rock in the deformed deeper depth (modified from Ref. [32]).

modulus) but are related to rock strength while the cutoff value between brittle and ductile range is not easy to determine due to the fact that the transition brittleness and ductility can be affected by numerous factors.

The fracability is about the quantification of ultimate rock strength, i.e., the rock failure. For hydraulic fracturing of tight reservoirs, the most important task is to determine whether the formation can be broken down under the designated pressure. In practice, the injectivity tests are usually performed to ensure the formation breakdown. The effective injectivity tests include but are not limited to diagnostic formation injection test (DFIT) and MiniFrac test (MF).

Hubbert and Willis [47] defined the breakdown pressure as:

$$P_b = 3\sigma_h - \sigma_H - P_p + \sigma_t \quad (15)$$

where σ_h is the minimum horizontal stress, σ_H is the maximum horizontal stress, P_p is the reservoir pore pressure, and σ_t is the rock tensile strength. Eq. (15) applies to the wellbore conditions in which the borehole wall is intact and impermeable, and the borehole wall effective tensile stress is less than the rock tensile strength.

From the MiniFrac tests, Raaen and Brady [48] recognized that higher injection pressure is required to breakdown the brittle formation than to breakdown the ductile formation (Fig. 28).

In the ductile breakdown of Fig. 28(b), the slope change of the bottom hole pressure (BHP) has been mostly interpreted as the indication of fracture initiation. Bai [49] considered it either as an indication of fracture initiation (i.e., LOP) or as the indication of ductile behaviour of rock failure (i.e., in the period of brittle–ductile transition). Bai [49] compared the pressure responses in the MiniFrac tests between the brittle formation and ductile formation as shown in Fig. 29 and provided the detailed calculation of various pressures under either brittle or ductile conditions.

In summary, fracability defines the degree of easiness to which a formation can be fractured. Generally speaking, fracability is related to the rock strength but can be associated with many other factors besides the rock strength. The following items can be considered as some key factors to identify the preferred perforation spots with high fracability:

- Small confinement
- Dominant elastic deformation

- Thermally enhanced (heating)
- Large permeability and porosity
- High density of natural fractures or micro fractures
- Not cemented
- No super seals
- Open fractures
- In tensile stress zone

Like brittleness, it is difficult to define the fracability by a single equation due to the influences of multiple factors. Based on the discussion in this paper especially aspired by the scenario illustrated in Fig. 24, the following simplified criteria are proposed to define the fracability for all practical purposes:

- No fracability: $F_b = 0$ where the breakdown pressure cannot be achieved during DFIT or MiniFrac tests.
- Maximum fracability: $F_b = 1$ where the breakdown pressure can be achieved and fracture extension has been verified during DFIT or MiniFrac tests.
- Variable fracability: $0 < F_b < 1$ according to the degree of easiness of obtaining the breakdown pressure. In particular:
 - Low fracability: $0 < F_b < 0.5$ where breakdown is ensured in the ductile formation but the fracture geometry is limited.
 - Average fracability: $F_b = 0.5$ where breakdown pressure is achieved.
 - High fracability: $0.5 < F_b < 1$ where breakdown pressure and fracture extension are achieved and the fracture geometry is sufficient.

Based on the discussion of this paper, the better fracability should be near the formation of lower confinement, and lower UCS. Fig. 30 shows the decreased fracability is related to the larger UCS and increased effective normal stress. Conversely, increased fracability is associated with the smaller UCS and decreased effective normal stress.

Employing the concept described in Fig. 30, the detailed UCS measured in the laminated shale/sand section can be used for identifying the effective injection intervals, as shown in Fig. 31 where the selected perforation locations are formation intervals with lower UCS and more fracable rocks. It should be emphasized that fracability is a dimensionless term which is a relative term with respect to the ease of fracturing.

The most fracable intervals are usually the weak spots which could be prone to excessive sand production. For shale gas reservoirs, this is usually not an issue. As a result, the preferred

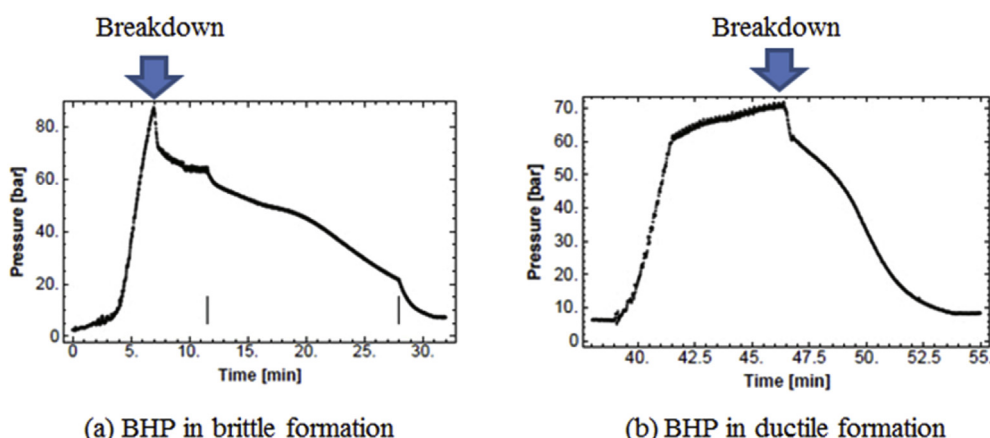


Fig. 28. Breakdown of brittle formation (a) and ductile formation (b) by injection [28].

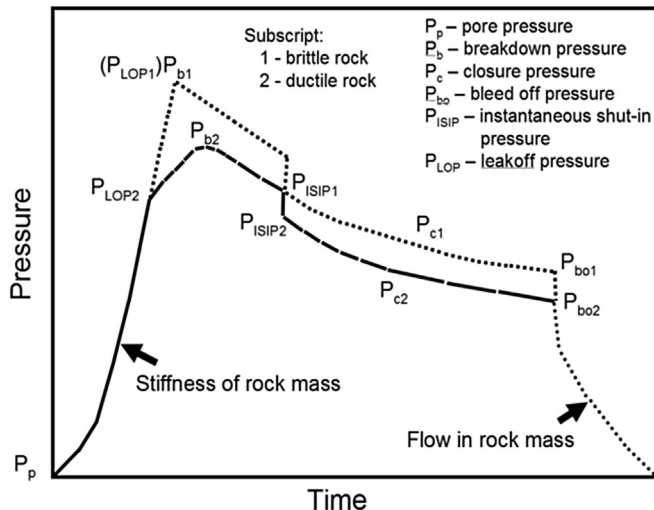


Fig. 29. Different pressure responses in the MiniFrac tests from the rocks with different properties [49].

perforation intervals are those relatively weak spots, as shown in Fig. 32.

6. Formation fracability – restricted fracturing

The formation breakdown scenario shown in Fig. 29 generally represents the formation fracturing under unconfined conditions. The examples of such conditions are: a) the hydraulic fracture grows out of payzone as a result of low stress contrast between the payzone and the bounding layers; and b) the fracturing occurs in the homogeneous formation where no permeability contrast between the perforated intervals and adjacent intervals can be identified.

In reality, unrestricted fracturing cases are rare since the free fracture extension can be frequently hindered as a result of: a) contained fracture growth within the payzone due to stress,

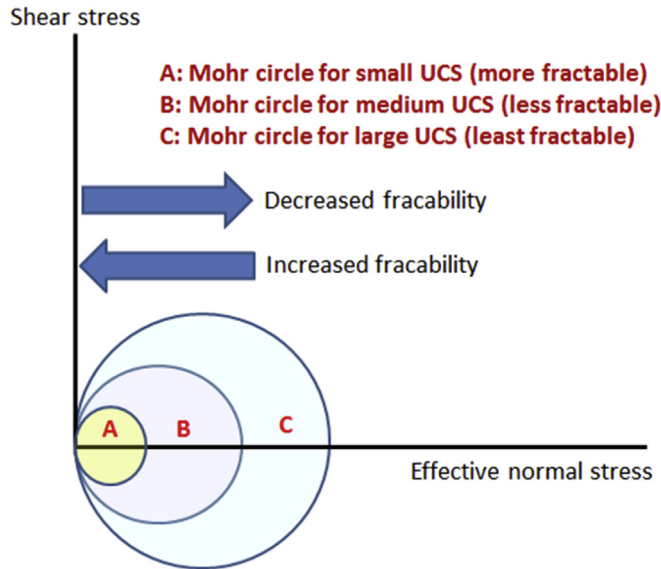


Fig. 30. Smaller UCS corresponds to larger fracability while greater UCS is related to decreased fracability.

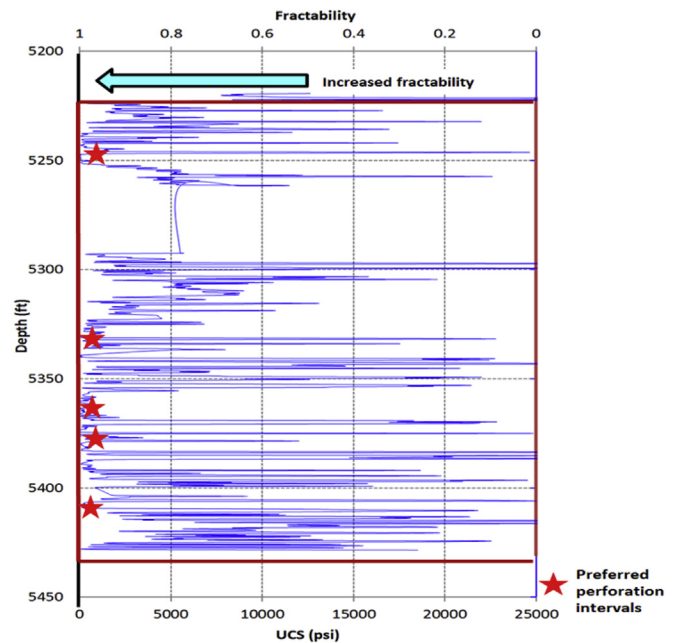


Fig. 31. Preferred perforation areas can be determined from the smaller UCS intervals, which is more fracable.

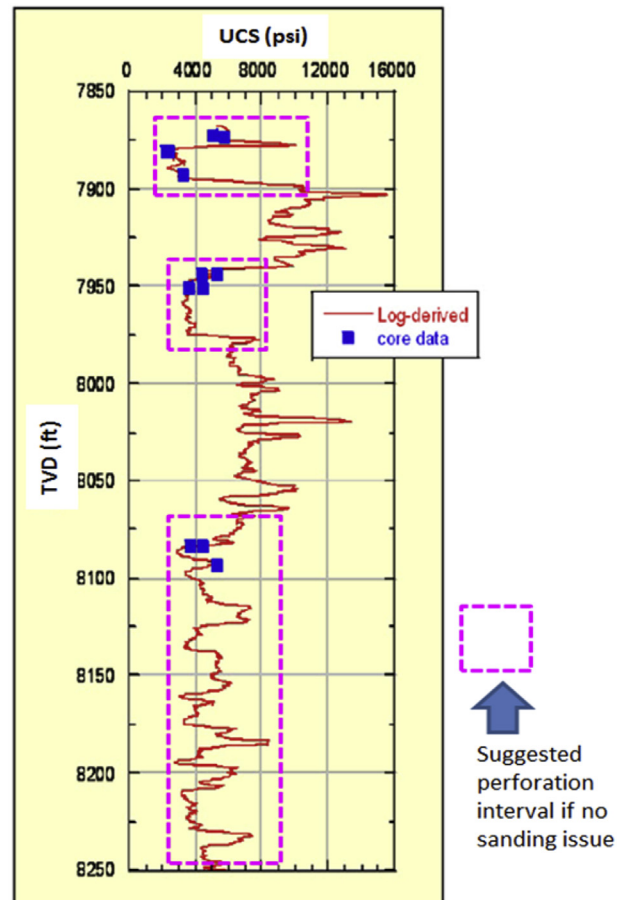


Fig. 32. Selecting desired perforation intervals from the weak spots.

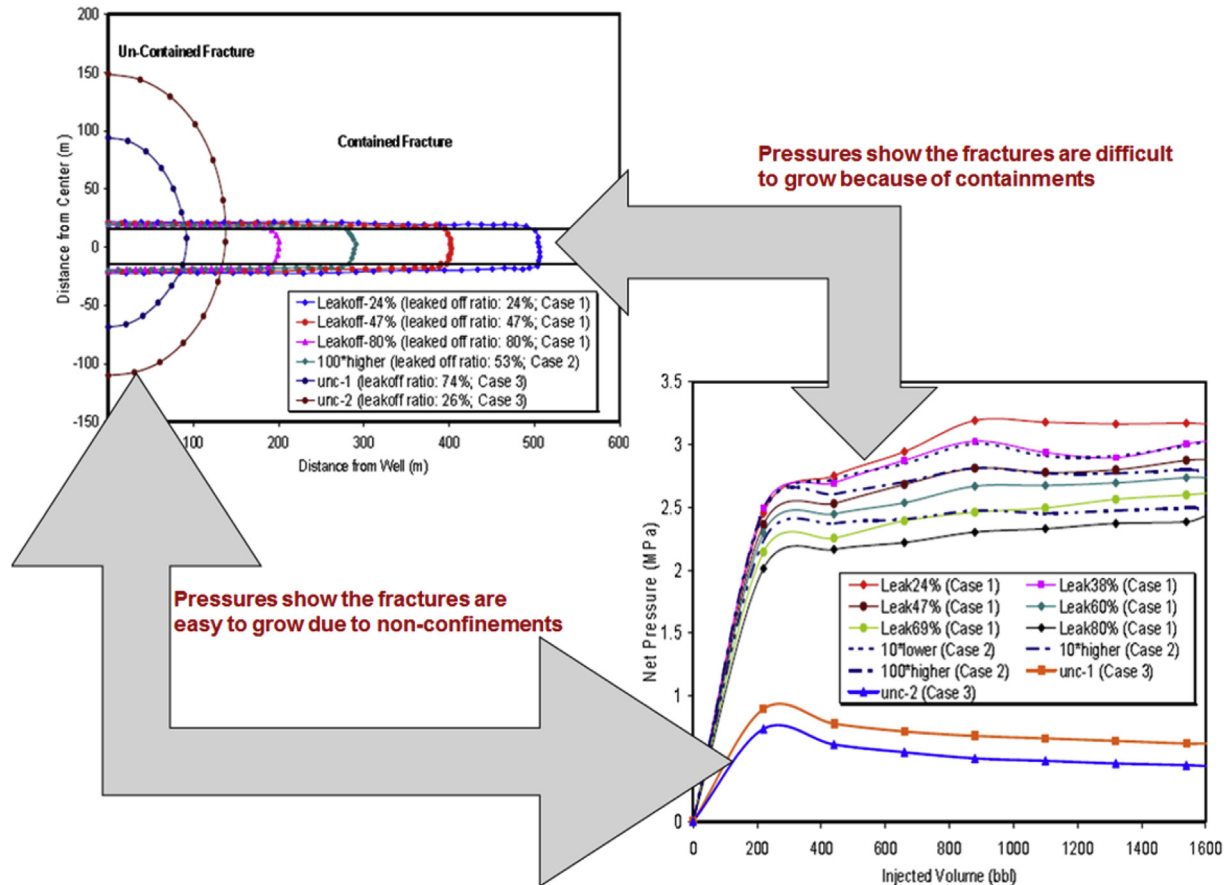


Fig. 33. Comparison between contained fracturing and uncontained fracturing with respect to fracture geometry and injection pressure [50].

modulus, or permeability contrasts between the payzone and the bounding formations; b) localized screen out that restricts the free fracture propagation; c) formation heterogeneities that form the discretized compartments of flow domains; and d) insufficient net pressure to extend the hydraulic fracture in the growing mode, etc.

Using the different signatures of bottom hole pressure responses during the injection (i.e., increasing pressure without obvious breakdown for contained fracturing and declining pressure with clear picture of formation breakdown for uncontained fracturing), Bai et al. [50] showed the geometric contrasts between the contained fracture growths within the payzone and uncontained penny shape fracture growths (Fig. 33).

For the restricted fracturing, the formation toughness plays a big role to reduce the fracture growth. Bai [49] provided a detailed relationship between breakdown pressure and fracture toughness. In fracture mechanics, the mode 1 fracture toughness K_{IC} represents the inherent ability of a material (e.g., a rock) to withstand a given stress field intensity at the tip of a fracture and to resist progressive tensile fracture extension.

For the hydraulic fracturing without using proppant, the fracture can be created only when the net pressure is sufficient to overcome the formation toughness. The net pressure is equal to the difference between the injection pressure and the closure stress. Papanastasiou [51] depicted the fracture propagation as a result of significant net pressure which exceeded the fracture toughness K_{IC} . As shown schematically in Fig. 34, the fracture grows when the fluid pressure exceeds the closure stress which creates positive net pressure and overcomes the fracture

toughness $K_i^{(+)}$. In contrast, the fracture shrinks when the fluid lag occurs in the fracture tip area which creates negative net pressure and fracture toughness $K_i^{(-)}$. The mode 1 fracture toughness K_{IC} is the summation of $K_i^{(+)}$ and $K_i^{(-)}$. Therefore, the fracture toughness is the critical rock strength value. If the positive net pressure exceeds this critical toughness value, the fracture will grow. Once the fracture grows bigger, the net pressure may consequently drop. As a result, the fracture will stop growing until the net pressure being increased to the level

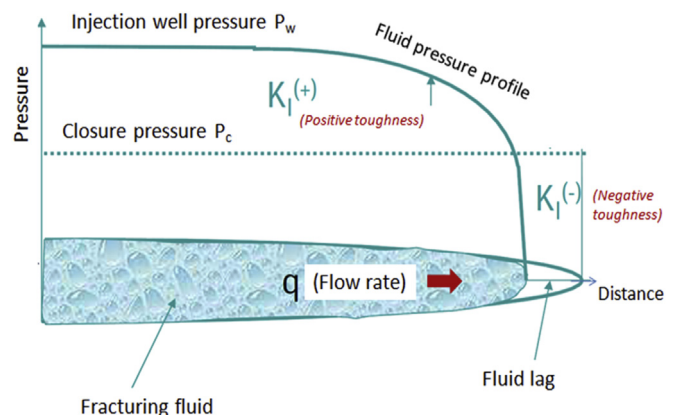


Fig. 34. The hydraulic fracture grows when the net pressure (i.e. $P_n = P_w - P_c$) is positive. The fracture shrinks in the region where the net pressure is negative. The resistance for the fracture growth is the fracture toughness [51].

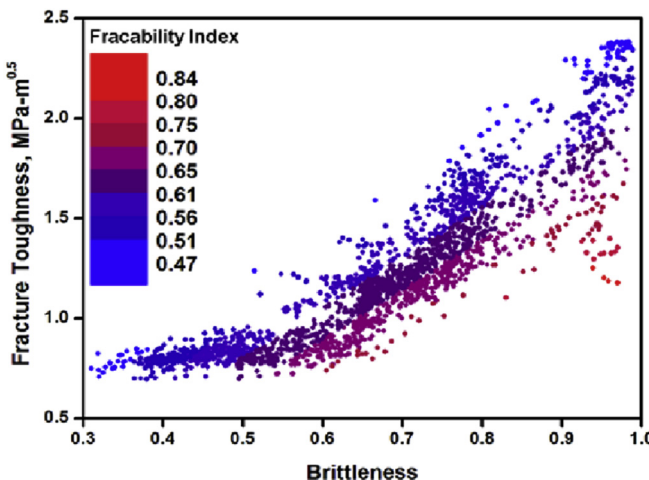


Fig. 35. Formation fracability chart from the relationship between fracture toughness and formation brittleness [17].

that again exceeds the fracture toughness. The dynamic process continues as long as the net pressure is continuously built up.

In Table 1, Jin et al. [17] defined the brittleness from the weight percentage of brittle silicate minerals (e.g., quartz, feldspar, and mica, or QFM) and brittle carbonate minerals (e.g., calcite and dolomite) while excluding the ductile clay minerals.

The fracability index from Jin et al. [17] is an arithmetic average of brittleness shown in Table 1 and fracture toughness, as indicated as follows:

$$FI = \frac{B_{QC} + K_{IC}}{2} \quad (16)$$

where K_{IC} is the mode 1 fracture toughness (i.e., tensile fracture).

Considering the rock with greater fracture toughness as one of the primary fracture barriers where the formation is less fracable, Jin et al. [17] provided fracability index chart from the cross plot between the fracture toughness and the normalized brittleness index, as shown in Fig. 35.

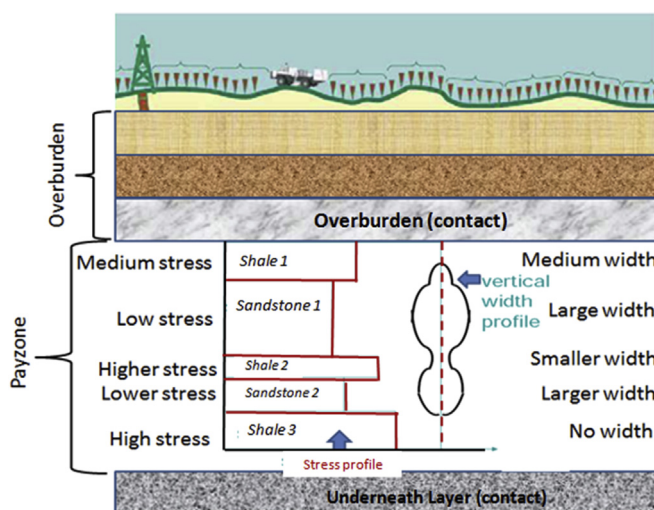


Fig. 36. Schematics showing smaller fracture width due to higher in-situ stress in shale layers and greater fracture width due to lower in-situ stress in sandstone layers from a hydraulic fracturing stimulation.

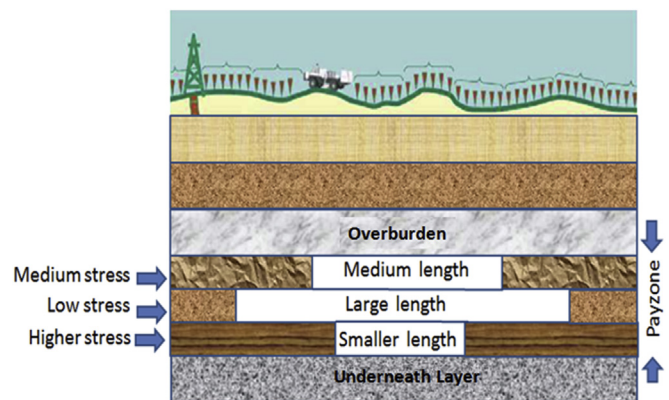


Fig. 37. Schematics showing smaller fracture length due to higher in-situ and greater fracture length due to lower in-situ stress from a hydraulic fracturing stimulation.

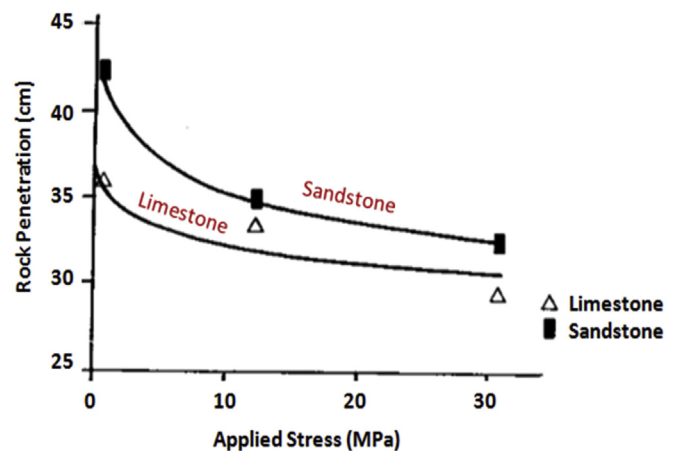


Fig. 38. Reversed relationship between rock penetration and applied stress [52].

It is seen from Fig. 35 that smaller fracability is associated with greater fracture toughness while the relationship between the toughness and the brittleness is nonlinear due to the additional influence of mineralogy on fracability shown in Eq. (16).

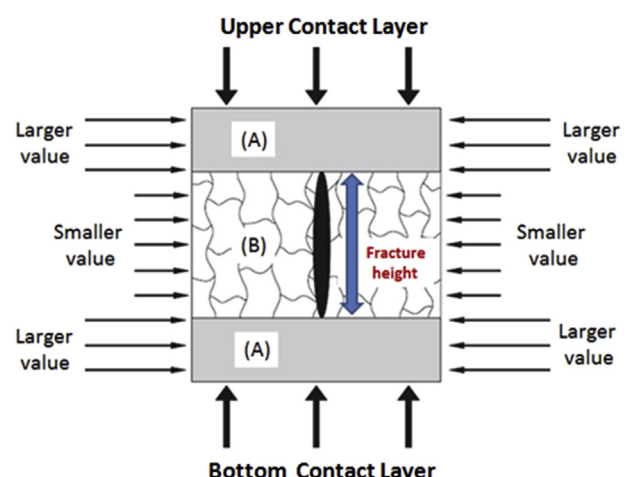


Fig. 39. Schematics showing the required sufficient contrasts to contain fracture height between layers (A) and (B) with respect to: a) stress, b) Young's modulus, and c) rock strength.

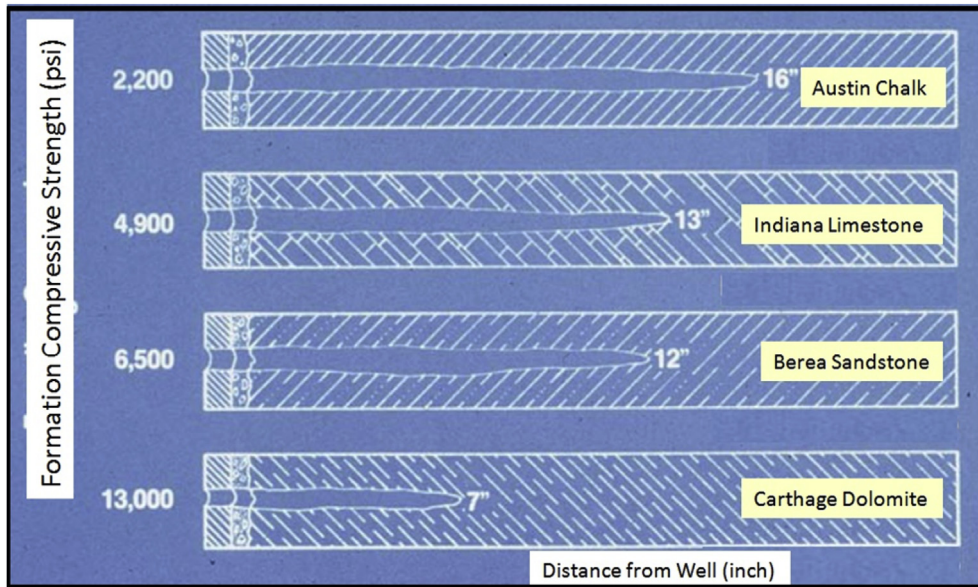


Fig. 40. Greater perforation penetration can be obtained in the rock with smaller compressive strength [53].

7. Verification of fracability

Rock fracability is related not only to the formation mechanical properties but also to the in-situ stress conditions of stimulated reservoir rocks. In the sedimentary rocks such as the laminated sandstone – shale sequences, shale is often subjected to the higher lateral stress than that of sandstone due to greater lateral rock strength. As described in Fig. 36, the stimulated wider fracture widths in sandstone layers and narrower fracture widths in shale layers are the result of the stress contrasts where the wider width corresponds to the lower stress and vice versa. In the hydraulic fracturing design for a vertical well, the fracture width is along the direction of minimum horizontal stress while the fracture length is parallel to the direction of maximum horizontal stress. Similarly to the case of fracture width, greater

stimulated fracture length can be achieved when the hydraulic fracture is subjected to the smaller lateral stress and vice versa, as depicted in Fig. 37.

The stress value also has an impact on the depth of perforation penetration. Based on the laboratory testing of various rocks, the reversed relationship between the applied stress and the rock perforation penetration depth was reported by Halleck et al. [52]; as shown in Fig. 38.

Based on the analysis of stress impact on the stimulated fracture geometry, it appears that most fracable formation intervals are those subjected to the lowest stress. Naturally, the stress is not the only factor that dictates the fracture geometry. Other mechanical contrasts such as formation Young's modulus and rock compressive strength also have significant impact on the stimulated fracture geometry. The fracture height

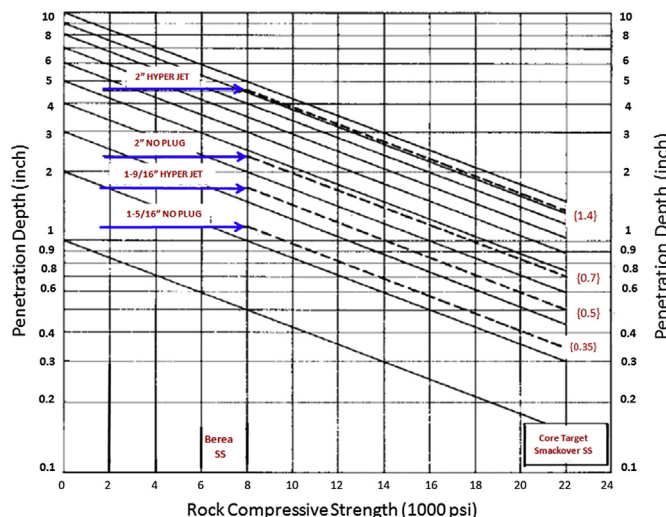


Fig. 41. Penetration depth is inversely related to rock compressive strength [54].

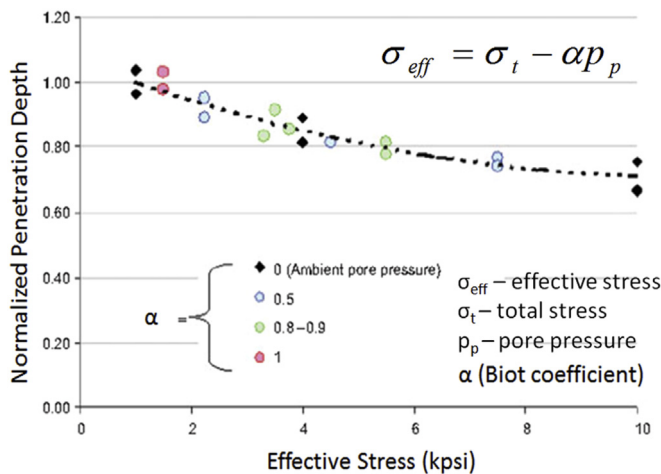


Fig. 42. Reversed relationship between penetration depth and effective loading stress [55].

containment can frequently be achieved if the mechanical contrasts (e.g., Young's modulus and rock compressive strength) are sufficiently large, as illustrated in Fig. 39.

Among other factors, the impact of rock compressive strength on reservoir stimulation has been recognized in the past. King [53] reported the perforation tests on various types of rocks that had different compressive strengths, as shown in Fig. 40 where the largest perforation length (or depth, 16") had been achieved on the Austin Chalk that had the lowest compressive strength (i.e., 2200 psi), which was in contrast to the smallest perforation length (7") on the Carthage Dolomite that had the highest compressive strength (i.e., 13,000 psi).

Weeks [54] provided the reverse relationship between the penetration depth and rock compressive strength (i.e., greater penetration depth related to smaller compressive strength)

based on the core testing in the normalized graph shown in Fig. 41.

As the rock strength can be defined from the subjected effective stress (i.e., difference between stress and pore pressure), Grove et al. [55] presented the reversed relationship between the perforation penetration depth and the in-situ effective loading stress, as shown in Fig. 42.

Generally speaking, the interval with higher rock strength is the barrier and the opposite is true (i.e., the interval with lower strength is the recommended perforation interval.). Fig. 43 shows an example of identifying barriers and fracable intervals in the shale reservoir. The carbonate interval (GR in Track 2) is identified as the barrier that should be avoided which has the higher strength (UCS in Track 4), greater density (RHOB in Track 5), and lower porosity (NPHI in Track 6). In contrast, the upper shale section is identified as the recommended fracable interval which has the lower strength (UCS in Track 4), smaller density (RHOB in Track 5), and greater porosity (NPHI in Track 6).

8. Conclusions

In the present study of stimulating unconventional shale gas reservoirs, the brittleness index profile along the reservoir payzone to identify the most desirable perforated intervals has become a common practice and has been considered as an indispensable geomechanics component in the approaches by the petro-physical domain. However, this paper challenges the validity of the brittleness index profiling method. The following conclusions are drawn as the result of the presented study:

- Formation brittleness and ductility are not related to the formation mechanical properties such as Young's modulus and Poisson's ratio as commonly used in the brittleness index profiling. Instead, formation brittleness and ductility are

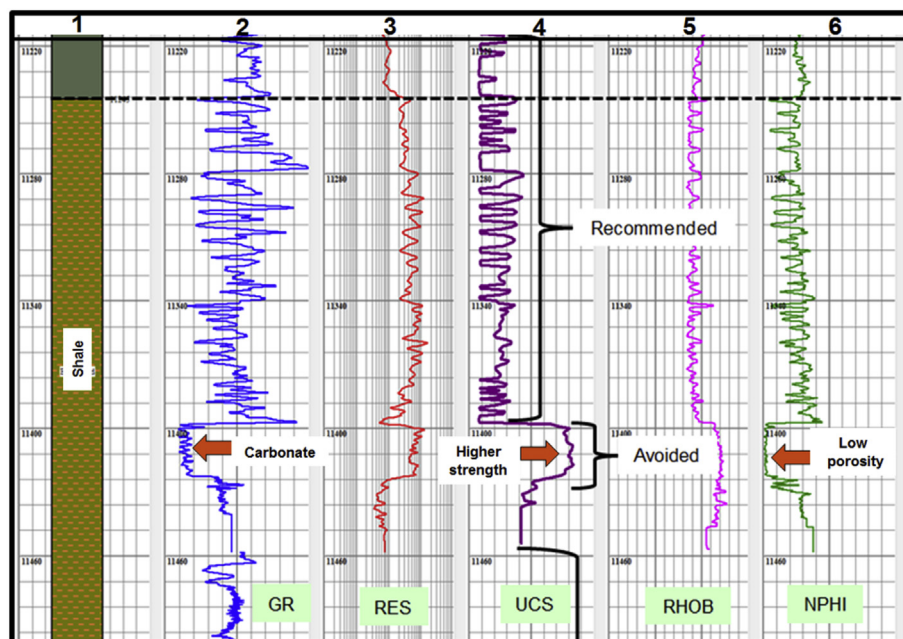


Fig. 43. Recommended perforation interval with lower rock strength and avoided perforation interval with higher rock strength in shale reservoir.

- related to the rock strength such as unconfined compressive strength (UCS) or fracture toughness.
- It is ambiguous to relate the formation brittleness to the formation fracability as brittle formation may have a greater rock strength under higher confinement that is more difficult to fracture, and vice versa.
 - The formation fracability is about the ultimate rock failure defined by the formation breakdown pressure. The breakdown pressure can be identified in the unrestricted fracturing. Unconfined compressive strength (UCS) is a good benchmark for the correlated breakdown pressure. However, it is difficult or sometime impossible to identify the breakdown pressure in the restricted fracturing since the fracturing is limited in size and is often localized while the extended free fracture propagation is not seen from the bottom hole pressure response. Under this condition, the formation fracability may be determined from the fracture toughness based dynamic fracturing process.
 - Disassociating formation brittleness from formation fracability allows us to correctly determine the most fracable formation intervals to perforate.
 - This paper proposes an effective approach to select the desirable stimulating intervals, i.e., select the weak spots determined from the formation UCS profile to establish the perforated intervals. The proposed method is supported by many early experimental studies.

References

- [1] S.A. Holditch, Tight gas sands, *JPT* 58 (6) (2006) 86–93. SPE 103356.
- [2] A.T. Zehnder, Fracture mechanics, in: Lecture Notes in Applied and Computational Mechanics, vol. 62, Springer Sci. & Business Media, 2012.
- [3] R. Rickman, M. Mullen, E. Petre, B. Grieser, D. Kundert, A practical use of shale petrophysics for stimulation design optimization: all shale plays are not clones of the Barnett shale, in: SPE 115258, SPE ATCE, Denver, CO, USA, Sept. 21–24, 2008.
- [4] D.B. Van Dam, P. Papamastasiou, C.J. de Pater, Impact of rock plasticity on hydraulic fracture propagation and closure, *SPE* 63172, in: SPER ATCE, Dallas, TX, USA, Oct. 1–4, 2002.
- [5] H.T. Alassi, R. Holt, O.-M. Nes, S. Pradhan, Realistic geomechanical modeling of hydraulic fracturing in fractured reservoir rock, CSUG/SPE 149375, in: Canadian Unconventional Conf., Alberta, CA, Nov. 15–17, 2011.
- [6] R. Romanson, R. Pongratz, L. East, M. Stanojcic, Novel, multistage stimulation processes can help achieve and control branch fracturing and increase stimulated reservoir volume for unconventional reservoirs, *SPE* 142959, in: SPE/Eupec/SPE ATCE, Vienna, Austria, May 23–26, 2011.
- [7] R.M. Holt, E. Fjaer, O.M. Nes, H.T. Alassi, A shaly look at brittleness, in: 45th US Rock Mechanics/Geomechanics Symposium, ARMA 11–366, San Francisco, CA, USA, June 26–29, 2011.
- [8] J.L. Miskimins, The impact of mechanical stratigraphy on hydraulic fracture growth and design consideration for horizontal wells, in: Search and Discovery Article #41102, Tulsa Geological Society Lunch Meeting, Nov. 27, 2012.
- [9] J.J. Zhang, L.R. Bentley, Factors determining Poisson's ratio, *CREWES Res. Rep.* 17 (2005).
- [10] R. Altindag, Correlation of specific energy with rock brittleness concepts on rock cuttings, *J. South Afr. Inst. Min. Metallurgy* 103 (3) (2003) 163–172.
- [11] H.K. Chiu, L.W. Johnston, The uniaxial properties of Melbourne mudstone, in: Proc. 5th Congr. ISRM, V.1, Melbourne, 1983, pp. A209–A214.
- [12] H.I. Inyang, Development of a preliminary rock mass classification scheme for near surface excavation, *Int. J. Surf. Min. Reclam.* 5 (1991) 65–74.
- [13] Y. Niwa, S.H. Kobayashi, Effect of couple-stresses distribution in specimens of laboratory tests, in: Proc. 3rd Congr. ISRM, V. 2, Denver, USA, 197–201, 1974.
- [14] J.B. Walsh, F.A. Brace, A fracture criterion for brittle anisotropic rock, *J. Geophys. Res.* 69 (1964) 3449–3456.
- [15] S. Kahraman, Correlation of TBM and drilling machine performances with rock brittleness, *Eng. Geol.* 65 (2002) 269–283.
- [16] D.M. Jarvie, R.J. Hill, T.E. Ruble, R.M. Pollastro, Unconventional shale-gas systems: the Mississippian barnett shale of north-central Texas as one model for thermogenic shale-gas assessment, *AAPG Bull.* 91 (4) (2007) 475–499.
- [17] X. Jin, S.N. Shah, J.C. Rogiers, Bo Zhang, Fracability evaluation in shale reservoirs – an integrated petrophysics and geomechanics approach, in: SPE Hydraulic Fracturing Technology Conference, Woodlands, TX, USA, 2014. SPE 168589.
- [18] H. Honda, Y. Sanada, Hardness of coal, *Fuel* 35 (1956) 45–461.
- [19] M. Protodyakonov, Mechanical properties and drillability of rocks, in: Proc. 5th Symposium on Rock Mech., The Univ. of Minnesota, USA, 1962.
- [20] G.E. Andreev, Brittle Failure of Rock Materials: Test Results and Constitutive Models, Taylor & Francis, 1995.
- [21] V. Hajabdolmajid, P. Kaiser, Brittleness of rock and stability assessment in hard rock tunneling, *Tunneling Undergr. Space Technol.* 18 (1) (2003) 35–48.
- [22] A.W. Bishop, Progressive failure with special reference to the mechanism causing it, in: Proc. Geotech. Conf., Oslo, 1967, pp. 142–150.
- [23] V. Hucka, B. Das, Brittleness determination of rocks by different methods, *Int. J. Rock Mech. Min. Sci. Geomech. Abstr.* 11 (10) (1974) 389–392.
- [24] B. Lawn, D. Marshall, Hardness, toughness, and brittleness: an indentation analysis, *J. Am. Ceram. Soc.* 62 (7–8) (1979) 347–350.
- [25] J. Sehgal, Y. Nakao, H. Takahashi, S. Ito, Brittleness of glasses by indentation, *J. Mater. Sci. Lett.* 14 (3) (1995) 167–169.
- [26] H. Copur, N. Bilgin, H. Tuncdemir, C. Balci, A set of indices based on indentation tests for assessment of rock cutting performance and rock properties, *J. South Afr. Inst. Min. Metallurgy* 103 (9) (2003) 589–599.
- [27] S. Yagiz, Assessment of brittleness using rock strength and density with punch penetration test, *Tunn. Undergr. Space Tech.* 24 (1) (2009) 66–74.
- [28] J.B. Quinn, G.D. Quinn, Indentation brittleness of ceramics: a fresh approach, *J. Mater. Sci.* 32 (16) (1997) 4331–4346.
- [29] F.P. Wang, J.F. Gale, Screening criteria for shale-gas system, *Gulf Coast Asso. Geol. Soc. Trans.* 59 (2009) 779–793.
- [30] D. Buller, S. Hughes, J. Market, E. Petre, D. Spain, T. Odumosu, Petrophysical evaluation for enhancing hydraulic stimulation in horizontal shale gas wells, SPE 132990, in: SPE Annual Technical Conference and Exhibition Held in Florence, Italy, 19–22 September, 2010.
- [31] L. Baron, B. Loguntsov, E. Pozin, Determination of the Properties of Rocks, Gosgortekhnizdat, Moscow, 1962.
- [32] J. Suppe, Principles of Structural Geology, Prentice-Hall, Eaglewood Cliffs, New Jersey, USA, 1985.
- [33] G.M. Ingram, J.L. Urai, Top-seal Leakage Through Faults and Fractures, the Role of Mudrock Properties, vol. 158, Geological Society, London, 1999, pp. 125–135.
- [34] H. Sone, M. Zoback, Mechanical properties of shale gas reservoir rocks – part 1: static and dynamic elastic properties and anisotropy, *Geophysics* 78 (5) (2013) 381–392.
- [35] H. Sone, M. Zoback, Mechanical properties of shale gas reservoir rocks – part 2: ductile creep, brittle strength, and their relation to the elastic modulus, *Geophysics* 78 (5) (2013) 393–402.
- [36] Y. Yang, H. Sone, A. Hows, M.D. Zoback, Comparison of brittleness indices in organic-rich shale formations, in: 47th US Rock Mech. Symposium, San Francisco, USA, June 23–26, 2013.
- [37] Ticona, Designing with Plastic, The Fundamentals, Ticona, Prod. Info. Services, Florence, KY, USA, 2000.
- [38] MPE (Modern Plastics Encyclopedia), The McGraw-Hill Companies, 1996.
- [39] J.A. Hudson, J.P. Harrison, Engineering Rock Mechanics – an Introduction to the Principles, Pergamon, Elsevier Science, Amsterdam, Netherland, 1997.
- [40] Wickham, Structural Geology, Chapter 5, Rheology, Univ. of Texas at Arlington, USA, 2012. GEOL 3443 course book.
- [41] S.J. Lutz, S. Hickman, N. Davatzes, E. Zemach, P. Drakos, A.R. Tait, Rock mechanical testing and petrologie analysis in support of well stimulation activities at the desert peak geothermal field, Nevada, in: Proc. 35th Workshop on Geothermal Reservoir Engineering, Stanford Univ., CA, USA, 2010.
- [42] A. Pagoulatos, Evaluation of Multistage Triaxial Testing on Berea Sandstone (M.S. Thesis), Univ. of Oklahoma, Norman, USA, 2004.
- [43] F. Ansari, Q. Li, High strength concrete subjected to uniaxial compression, *ACID Mater. J.* (1998).
- [44] X. Lu, Uniaxial and Triaxial Behavior of High Strength Concrete with and without Steel Fibers (Ph.D. Dissertation), New Jersey Institute of Technology, USA, 2005.
- [45] M. You, Strength and damage of marble in ductile failure, *J. Rock Geotech. Eng.* 3 (2) (2011) 161–166.
- [46] S.H. Kirby, Tectonic stresses in the lithosphere: constraints provided by the experimental deformation of rocks, *J. Geophys. Res.* 85 (1980) 6353–6363.
- [47] M.K. Hubbert, D.G. Willis, Mechanics of hydraulic fracturing, *Trans. SPE-AIME* 210 (1957) 153–168.
- [48] A.M. Raaen, M. Brady, Pump in/flowback tests reduce the estimate of horizontal in-situ stress significantly, SPE 71367, in: SPE Annual Technical Conference and Exhibition, New Orleans, USA, 30 September–3 October, 2001.
- [49] M. Bai, Risk and uncertainties in determining fracture gradient and closure pressure, in: 45th US Rock Mechanics/Geomechanics Symposium, San Francisco, CA, June 26–29, 2011, pp. 11–132.
- [50] M. Bai, S. Green, R. Suarez-Rivera, Effect of leakoff variation on fracturing efficiency for tight shale gas reservoirs, in: Proc. 40th U.S. Rock Mechanics Symposium, Anchorage, Alaska, USA, 2005.

- [51] P. Papanastasiou, *Hydraulic Fracturing: Basic Concepts and Numerical Modeling*, Dept. of Civil and Environmental Eng., Univ. of Cyprus, Cyprus, 2002.
- [52] P.M. Halleck, R.J. Saucier, L.A. Behrmann, T. Ahrens, Reduction of jet perforator penetration in rock under stress, in: SPE 63th ATCE, SPE 18245, Houston, TX, USA, 1988.
- [53] G.E. King, *Perforation Basics – How the Perforating Processes Work*, 2009. George E. King Engineering.
- [54] S.G. Weeks, Formation damage or limited perforation penetration? Test well shooting may give a clue, *J. Petroleum Technol.* (1974) 979–984.
- [55] B. Grove, J. Heiland, I. Walton, D. Atwood, Drilling and completion, *SPE J.* (2009) 678–685.